CHAPTER II

ASTABLE OSCILLATOR NETWORK

The basic building block of bioinspired oscillatory networks is the oscillator. However, this term involves a large set of elements that share the property of varying one of their variables above and below a mean value. To build an oscillatory network that can segment images, as the ones presented in the previous chapter, certain kind of oscillators with some synchronization properties are needed.

The main efforts in studying oscillators applied to these networks have been focused in mimicking biological phenomena using relaxation oscillators. They were first introduced in 1926 by van der Pol [van der Pol'26] using an electronic circuit. Their main characteristic is that they have two distinct time scales: a fast one and a slow one. These oscillators have similarities to biological cells and neurons have been modeled using the models [Fitzhugh, 61] [Nagumo et al., 62] [Morris and Lecar'81] that were a simplification of a squid's giant axon modeled in [Hodgkin and Huxley'52]. Further simplifications led to the integrate-and-fire model. This model is a gross approximation of neural activity, however its dynamics is rich enough to provide a heuristic model for neurobiology.

Synchronizing and computational properties of pulse-coupled oscillators, which interact with short pulses, have also been studied in different papers, especially their

advantages over linear or harmonic oscillators, which interact during the whole oscillation cycle [Somers and Kopell'93]. Synchronization phenomena are widespread in nature. A rich collection of examples of biological oscillators and their synchronization is the book of Winfree [Winfree'80] who considered that oscillators are strongly attracted to their limit cycles, thus, amplitude variations can be neglected and only phase variations need to be considered. In addition to this, in 1975, Peskin [Peskin'75] introduced a model of pulse-coupled oscillators for cardiac pacemaker cells and proved synchronization for two coupled oscillators. Later, in 1990, Mirollo and Strogatz [Mirollo and Strogatz'90] demonstrated that global synchronization for this model with any number of oscillators could be achieved. However, their analysis is restricted to a certain class of networks that consist of identical oscillators, equal weights, equal frequencies and strictly concave down functions. Later, Senn and Urbanczik [Senn and Urbanczik'00] showed that for non-leaky integrate and fire oscillators and almost all networks with weak homogeneity, cells synchronize for all initial conditions. A more general analysis can be found at [Hopfield and Herz'95], where different models of integrate-and-fire cells and network structures with local and global connections are studied. They conclude that even simple locally coupled integrate-and-fire neurons are able to encode objects by synchronized firing patterns and architectures that include longer-range connections and inhibitory synapses are able to perform specific computations. Campbell et al. [Campbell et al.'99] demonstrated these computational properties for image segmentation.

Synchronizing properties of relaxation oscillators are similar to integrate-and-fire characteristics. Most of the models that demonstrate synchronization of oscillator networks use long-range connections to achieve phase synchrony. However, some authors demonstrated analytically and by computer simulations, that synchronization can be achieved with local connections for different kinds of relaxation oscillators. Somers and Kopell [Somers and Kopell'93] [Somers and Kopell'95] studied coupled oscillators via Fast Threshold Modulation (FTM) and demonstrated that this coupling leads to synchrony faster than phase pulling in harmonic oscillators. They also studied boundary effects in chains of oscillators and variations in oscillator frequencies. Izhikevich [Izhikevich '00] completed the previous analysis with weakly connected oscillators using phase equations. Wang and Terman [Wang and Terman'95] [Terman and Wang'95] added Selective Gating to FTM, a mechanism that selectively desynchronizes oscillators via a global cell. Combining both mechanisms, they used their network for image segmentation and obtained successful results, even for real world images [Wang and Terman'97]. Dragoi and Grosu [Dragoi and Grosu'98] developed a rigorous mathematical study of synchronization in a network of FitzHugh-Nagumo oscillators.

In addition to synchronizing, oscillators under strong coupling may develop a stable equilibrium state where there is no oscillation. Ermentrout and Kopell [Ermentrout and Kopell'90] analyzed it and showed that weak couplings will not lead to this equilibrium state. They also suggested that delays could prevent oscillatory death.

Delays are an important issue in oscillation synchronization, especially when applied to physical systems. Compared to computer simulations that can add any delay or avoid it, delays in physical systems are unavoidable. This issue and its effects on network computing abilities have not been widely studied yet, although interest is growing due to its applications. Campbell and Wang [Campbell and Wang'98b] studied this issue for a specific kind of oscillators and Fox et al. [Fox et al.'01] presented a method to reduce phase-lag when delays are caused by slow synapses.

In this chapter, we focus on a network made of astable oscillators with scene segmentation capabilities. Astable oscillators are relaxation oscillators that can be very easily implemented using microelectronic hardware. However, they are difficult to analyze with closed mathematical expressions due to their piecewise nature and specially if second-order device models are considered. Dynamics of ideal astable oscillators have been studied in [Varigonda and Georgiou'2000] and [Georgiou'97] under a mathematical perspective. However, their analysis is focused on oscillator synchrony and not to applications of synchronized oscillators. In addition to this, ideal models must be modified to model non-idealities of physical systems

Next sections will show the ability of a network of astable oscillators with secondary effects similar to that produced by integrated devices to successfully segment scenes.

First, an ideal model of oscillator is presented. Its characteristics are studied analytically and numerically as the behavior of two coupled ideal oscillators. The effects of negative coupling and mismatch are also studied.

Secondly, a more complex model is analyzed. This model takes into account the delay at the output of the oscillator. It is compared to the ideal oscillator and we give an equivalency between them. Numerical simulations show the behavior of two positively and negatively coupled oscillators and the effects of mismatch.

In the third place, we simulate the behavior of 1-dimensional and 2-dimensional networks of oscillators and its dependency of different parameters.

Finally, we show a network that can successfully segment simple images and some conditions that it must accomplish for this.

II.1 OSCILLATORY SEGMENTATION SCHEME

The scheme presented in this chapter is based on an algorithm developed by Wang and Terman [Wang and Terman'95] [Terman and Wang'95]. This algorithm, called LEGION (Locally Excitatory Globally Inhibitory Oscillator Network), consists of a 2-dimensional network of relaxation oscillators locally connected with positive coupling and a global cell negatively coupled to all oscillators. Each oscillator is associated with a characteristic of the input scene (e.g. pixel intensity, motion, pre-processed acoustic components) (Figure II.1) and after the segmentation process concludes, characteristics that belong to the same object are grouped together -objects are groups of pixels that share the same characteristic (black or white in this case) that are spatially connected to each other. This binding information is coded in oscillator phases (Figure II.2). More

specifically, oscillators that are mapped to the same object are active simultaneously while others are silent. For the sake of simplicity, simple luminance images with each pixel connected to one oscillator are used in this work.

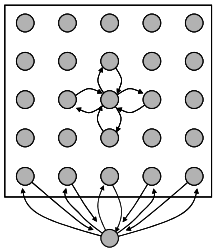

Figure II.1: Network structure. Each circle represents a cell. Only excitatory center cell connections and bottom line cell connections to inhibitor are shown for clarity.

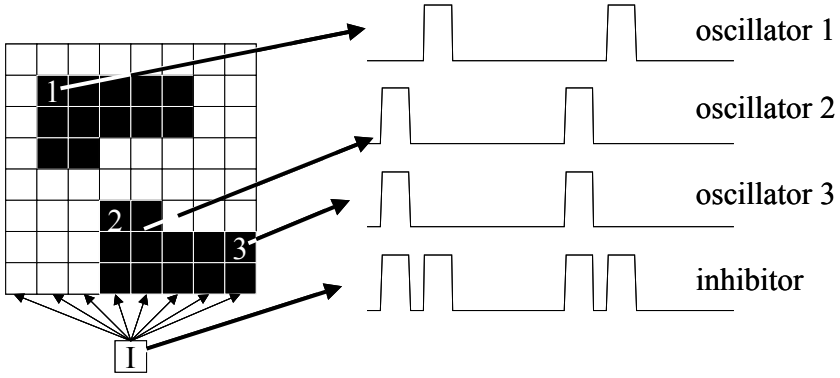

Figure II.2: Example of network oscillatory behavior. Oscillators 2 and 3 are associated with pixels that belong to the same object and oscillate in phase. Oscillator 1 is associated with a pixel that belongs to a different object; thus, it oscillates at the same frequency but with a different phase. Global inhibitor behavior is also shown at the lower time diagram. It is active when any oscillator in the network is active.

The basic block of the LEGION network is the relaxation oscillator. The exact equation that gives the temporal behavior of the oscillator is not important provided it has some basic properties [Somers and Kopell'95]. Different equations have been used but the most common ones for LEGION are given below:

$$\frac{dx_i}{dt} = 3x_i - x_i^3 + c - y_i + S_i + \rho$$
$$\frac{dy_i}{dt} = \varepsilon\left(\gamma\left(1 + \tanh\left(x_i / \beta\right)\right) - y_i\right) \qquad \text{Eq. II.1}$$

Oscillator (i) is defined as a feedback loop between a fast excitatory unit (x_i) and a slow inhibitory unit (y_i). S_i represents excitatory and inhibitory synapses from nearest neighbors of oscillator i and from the global cell. ρ is the noise, a necessary term to

apply a random component to the system strong enough to desynchronize oscillators that do not belong to the same object. Obviously, this term should be included when simulating the equation system on a digital computer because digital operations only include very small truncating errors, however, it is not necessary in a physical analog implementation due to mismatch and real noise. Finally c, ε, γ and β are constants that can be fixed for different oscillation parameters.

Excitatory synapses are positive couplings between adjacent cells. If two cells are close enough and have a similar characteristic (both are black or white in a monochrome image or have similar luminance level in a gray level image), an excitatory connection is established. When a cell goes active, that is to say, its x variable has a high value, its output synapses excite all cells that have an excitatory connection. On the other hand, when a cell is not in its active state (x has a low value), synapse values are null.

Note that total excitation may differ depending on the number of excitatory oscillators that are connected to a cell and it can affect basic oscillator characteristics as frequency. As an example, a corner cell may have only two exciting connections while a center cell may have four. Thus, to help synchrony, excitatory synapses are normalized so the sum of all excitatory terms for a particular cell when all neighbor cells are active is constant throughout the network.

$$S_{ij,exc} = \frac{S_{exc}}{n}; \qquad j = 1..n \qquad \text{Eq. II.2}$$

where $S_{ij,exc}$ is the excitatory synapse value contributed by cell j to cell i and n is the number of coupled cells to cell i.

Inhibitory synapses are negative couplings that affect all cells and their value depends on the state of a global cell or global inhibitor. This cell reflects the state of the whole network and it becomes active when any cell of the network is active. The aim of this cell is to desynchronize blocks of oscillators that not belong to the same object.

As stated above, the exact form of the oscillator non-linear function is not crucial for its segmentation properties. Thus, next we present a different oscillator model from Eq. II.1 that can be easily implemented on a microelectronic circuit.

II.2 THE BASIC IDEAL OSCILLATOR

III.2.1 SINGLE OSCILLATOR

The astable oscillator will be modeled as a damped integrator and a hysteresis comparator (Figure II.3). First, we will assume that the comparator is very fast so no dynamic behavior should be considered and we will refer to it as a basic ideal oscillator.

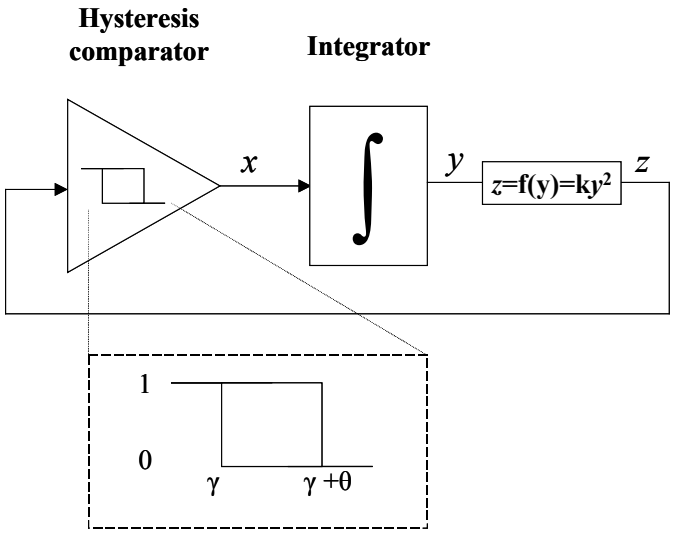

Figure II.3: Basic oscillator built of a hysteresis comparator and a damped integrator

The basic ideal oscillator is composed of a hysteresis comparator that compares the input variable z with thresholds γ and γ+θ. Then its output x, which can take values 0 or 1, is integrated by the damped integrator as defined in Eq. II.3(a) and (b). Output of the integrator, y, is transformed by a non-linear function f defined in Eq. II.3(c). Result, z, is the input of the comparator and closes the loop.

$$\begin{cases} \dfrac{dy}{dt} = -q & x = 0 \quad (a) \\ \dfrac{dy}{dt} = p; & x = 1 \quad (b) \\ z = f(y) = ky^2 & (c) \end{cases} \qquad \text{Eq. II.3}$$

Parameters p, q and k are constants. To simplify notation, in this analysis we will also refer to equivalent thresholds for y state variable. Thus, values of y that change comparator's output are Γ, low threshold, and $\Gamma+\Theta(\gamma)$, high threshold. Notice that hysteresis cycle width in the y-domain (Θ) depends on z-thresholds, width and position, due to y-z quadratic relation (Eq. II.4). To explicitly show that dependency we use notation: $\Theta(\gamma)$.

$$\begin{aligned} & f^{-1}(\gamma) = \sqrt{\frac{\gamma}{k}} = \Gamma \\ & f^{-1}(\gamma+\theta) = \sqrt{\frac{\gamma+\theta}{k}} = \Gamma + \Theta(\gamma) \Rightarrow \\ & \Rightarrow \Theta(\gamma) = f^{-1}(\gamma+\theta) - f^{-1}(\gamma) = \sqrt{\frac{\gamma+\theta}{k}} - \sqrt{\frac{\gamma}{k}} \end{aligned} \qquad \text{Eq. II.4}$$

Time evolution and orbit of the oscillator are shown in Figure II.4. As dynamics of the comparator is very fast, changes of x are considered immediate, which is shown in the orbit by two arrows.

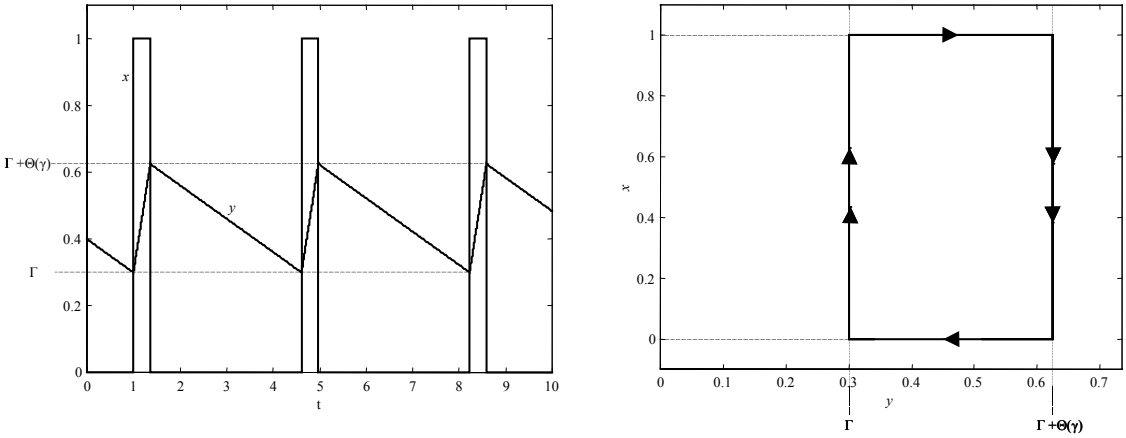

Figure II.4: Temporal behavior and orbit of a single ideal oscillator. Parameters are: γ=0.3, θ=1, p=0.9, q=0.1, k=3.33. Arrows indicate the evolution of state variables through time in the orbit. Note that two arrows indicate fast dynamics when x shifts from 0 to 1 and backwards.

The oscillator is said to be in its active state when its output (x) is high, and in the silent state, when its output is low.

Basic characteristics of this oscillator, as x frequency (f_0) and duty cycle (Δ), can be easily calculated and are shown in Eq. II.5.

$$\begin{cases} f_0 = \dfrac{pq}{\Theta(\gamma)(p+q)} & (a) \\ \Delta = \dfrac{q}{p+q} & (b) \end{cases} \qquad \text{Eq. II.5}$$

where $\Theta(\gamma)$ is the range of y.

II.2.2 TWO COUPLED OSCILLATORS

Now, we will consider two coupled oscillators linked via excitatory connections or synapses and we will refer to them as A and B. The purpose of excitation is mutual synchronization of cells. These connections couple one oscillator to the other and they consist in shifting both thresholds of the hysteresis cycle of the excited oscillator to higher currents when the exciting oscillator is active. Thus, excited cycle thresholds have been increased by s and they are γ+s and γ+θ+s, which correspond to y-thresholds Γ+$S(\gamma)$ and Γ+$\Theta(\gamma)$+$S(\gamma$+$\theta)$ respectively (Figure II.5). Notice that excitation on y-domain depends on both hysteresis thresholds γ and γ+θ (Eq. II.6).

$$f^{-1}(\gamma+s)=\sqrt{\frac{\gamma+s}{k}}=\Gamma+S(\gamma)\Rightarrow S(\gamma)=f^{-1}(\gamma+s)-f^{-1}(\gamma)=\sqrt{\frac{\gamma+s}{k}}-\sqrt{\frac{\gamma}{k}}$$
$$f^{-1}(\gamma+\theta+s)=\sqrt{\frac{\gamma+\theta+s}{k}}=\Gamma+\Theta(\gamma)+S(\gamma+\theta)\Rightarrow \qquad \text{Eq. II.6}$$
$$\Rightarrow S(\gamma+\theta)=f^{-1}(\gamma+\theta+s)-f^{-1}(\gamma+\theta)=\sqrt{\frac{\gamma+\theta+s}{k}}-\sqrt{\frac{\gamma+\theta}{k}}$$

If the excited oscillator is not far from changing to its active state, it becomes also active immediately or after a short time and excites the other oscillator. Then, both cells have their *z*-thresholds shifted *s*.

When one oscillator goes back to its silent state, it stops exciting the other cell. If excitation has not produced any effect during the active period (i.e. the other cell has not jumped to active), it is 'forgotten' because the hysteresis cycle of the excited cell goes back to its original state.

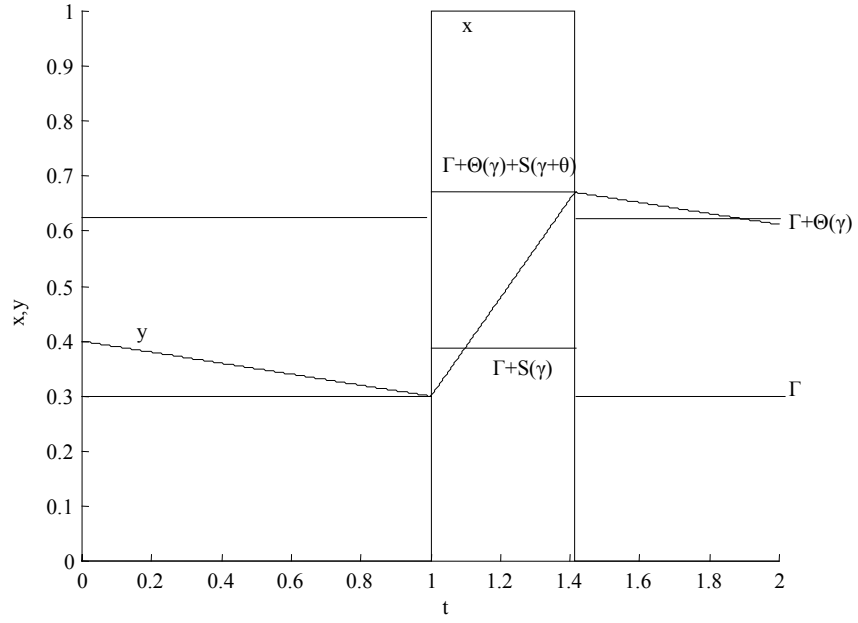

Figure II.5: Temporal evolution of one oscillator coupled to another synchronous oscillator. *y* thresholds are shifted *S(γ)* and *S(γ+θ)* during the active phase due to coupling. Notice that modifying thresholds only affects oscillators that shift to active during excitation and not afterwards.

II.2.2.1 Identical Oscillators

The first case we present is when both oscillators are identical but they start their oscillation with different initial conditions. Depending on these initial conditions, their evolution differs. We also assume that the duty cycle is smaller than 50% thus $p>q$. This condition is required in segmentation applications because as many active cycles should fit in one silent cycle as objects are to be segregated.

As astable oscillators are not linear oscillators, phases are not defined. However, we can define a magnitude that quantifies synchronization and it is time. However, as timescales are different in the silent state and the active state, only magnitudes when both oscillators are in the same state are meaningful. This magnitude, let's call it τ, is the time the trailing oscillator (the one that is going to shift its comparator the last) takes to reach the same state (y and x) as the leading oscillator (the one that shifted to active the first). Thus, $y_{Leading}(t_0)=y_{Trailing}(t_0+\tau)$ and $x_{Leading}(t_0)=x_{Trailing}(t_0+\tau)$.

Furthermore, the integrator presented in this model is charged and discharged linearly with time, thus it is equivalent to talk about the difference of their integrator output variables ($\Delta y=y_B-y_A$) and the time (τ) it takes the trailing oscillator to reach the value of the leading one because they are proportional.

When oscillators do not change their state, that is to say they do not jump from the active state to the silent state or vice versa, there is no variation of Δy. Thus, changes occur only when one oscillator shifts its state.

From silent state to active state:

First, let's consider that y-variable of oscillator A (y_A) is lower than y-variable of B (y_B) and both of them are in the silent state ($x_A=x_B=0$), thus both y are decreasing at a constant rate q.

Case S1:

When y_A decreases and reaches Γ at time $t=t_0$, oscillator A changes its state and gets active immediately after this ($x_A(t_0+\delta)=1$ where $\delta\rightarrow 0$). Since oscillator A is now active, it excites oscillator B by shifting its threshold from Γ to $\Gamma+S(\gamma)$ If $x_B(t_0)$ is smaller than threshold $\Gamma+S(\gamma)$, oscillator B will also change its state to active immediately and Δy will not vary (Figure II.6). In spite of y_A and y_B not being equal, the difference cannot be detected looking at x because their behavior is identical and oscillators can be considered synchronized.

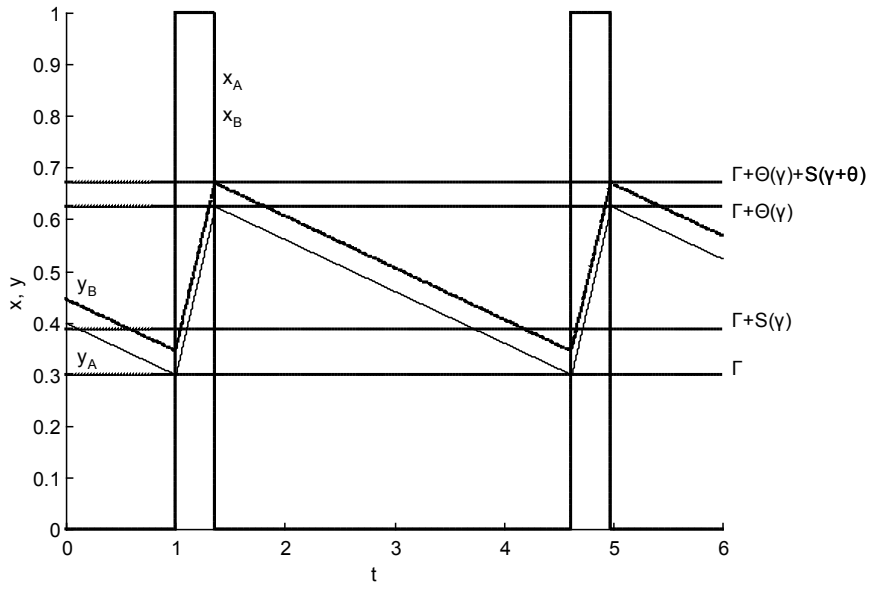

Figure II.6: Temporal evolution of two oscillators *A* and *B*. Integrator voltage difference is not equal but they can be considered synchronized because both shift from active to silent state and vice versa simultaneously. Equivalent voltage thresholds are also depicted. Parameters used are γ=0.3, θ=1, S=0.2, q=0.1, p=0.9, k=3.33.

Case S2:

However, if oscillator *A* shifts to active state and oscillator *B* does not immediately because $y_B(t_0)>\Gamma+S(\gamma)$, integrator output variables will not change at the same time and the difference $\Delta y(t)=y_B(t)-y_A(t)$ can be reduced under certain conditions and synchronize in next cycles.

Let's assume that initial conditions lead oscillator *B* to jump to active state at $t=t_1$ and $y_A(t_1)<y_B(t_1)$, as depicted in Figure II.7. Initial conditions at time $t=t_0$ are $y_A(t_0)=\Gamma$, $y_B(t_0)=y_{B0}$; and at $t=t_1$, they are $y_A(t_1)=y_{A1}$, $y_B(t_1)=\Gamma+S(\gamma)$. Then, Eq. II.7 shows the evolution of y-variable of both oscillators for $t_0<t<t_1$.

$$\begin{cases} y_A(t) = \Gamma + p(t-t_0); & t_0 \le t \le t_1 \quad (a) \\ y_B(t) = y_{B0} - q(t-t_0); & t_0 \le t \le t_1 \quad (b) \end{cases} \qquad \text{Eq. II.7}$$

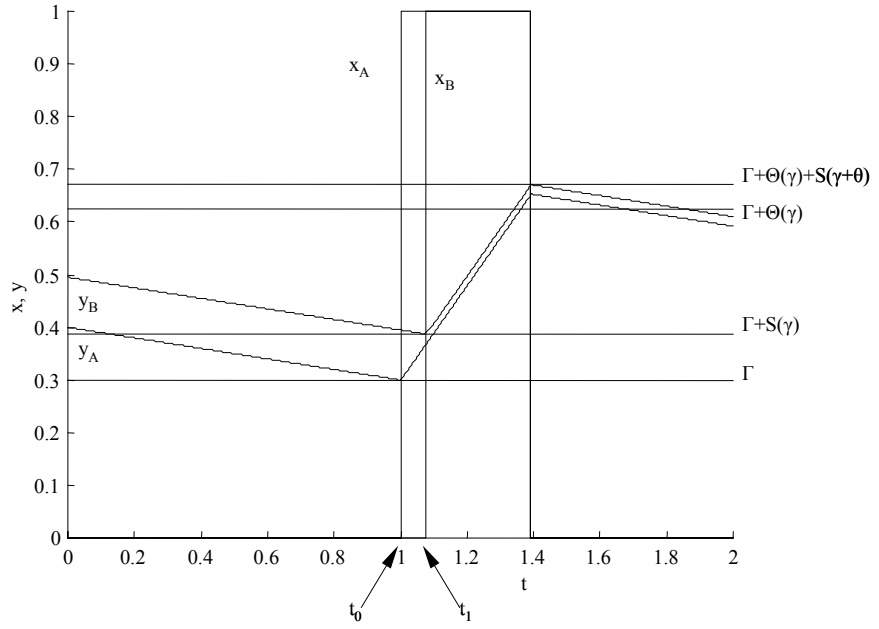

Figure II.7: Temporal evolution of two oscillators *A* and *B*. Integrator voltage difference is reduced after the first jump to the active state.

As we know the final condition of y_B ($y_B(t_1)=\Gamma+S(\gamma)$), we calculate the value of $(t-t_0)$ from Eq. II.7(b):

$$\Gamma + S(\gamma) = y_B(t_1) = y_{B0} - q(t_1 - t_0) \Rightarrow (t_1 - t_0) = \frac{y_{B0} - (\Gamma + S(\gamma))}{q} \qquad \text{Eq. II.8}$$

Finally, using Eq. II.7 and Eq. II.8 we calculate the variation of Δy, which is equivalent to phase difference in linear oscillators and it is a good estimation of mutual synchronization.

$$\begin{aligned} \Delta y(t_1) = y_B(t_1) - y_A(t_1) = y_{B0} - \Gamma - (p+q)(t_1 - t_0) = \\ = \Delta y(t_0) - \left(1 + \frac{p}{q}\right)(y_{B0} - \Gamma - S(\gamma)) \end{aligned} \qquad \text{Eq. II.9}$$

Also, as $\Delta y(t_0)=y_B(t_0)-\Gamma$:

$$\Delta y(t_1) = \Delta y(t_0) - \left(1 + \frac{p}{q}\right)(\Delta y(t_0) - S(\gamma)) \qquad \text{Eq. II.10}$$

The upper limit for these conditions is $\Delta y(t_1)=0$, i.e. $y_A(t_1)=y_B(t_1)=\Gamma+S(\gamma)$, when perfect synchronization occurs at the next oscillation cycle. Thus, from Eq. II.10, we can state that the initial condition that leads to perfect synchrony is:

$$\Delta y(t_0) = \left(1 + \frac{q}{p}\right) S(\gamma) \qquad \text{Eq. II.11}$$

Note that, under assumed conditions, $S(\gamma) < \Delta y(t_0) < (1+q/p)S(\gamma)$ the bigger $\Delta y(t_0)$ is, the bigger is the reduction of Δy and always $\Delta y(t_0) > \Delta y(t_1)$

Case S3:

When $\Delta y(t_0)$ exceeds condition of Eq. II.11, $\Delta y(t_1)$ changes its sign ($y_A(t_1)>y_B(t_1)$), but Eq. II.9 and Eq. II.10 are still valid.

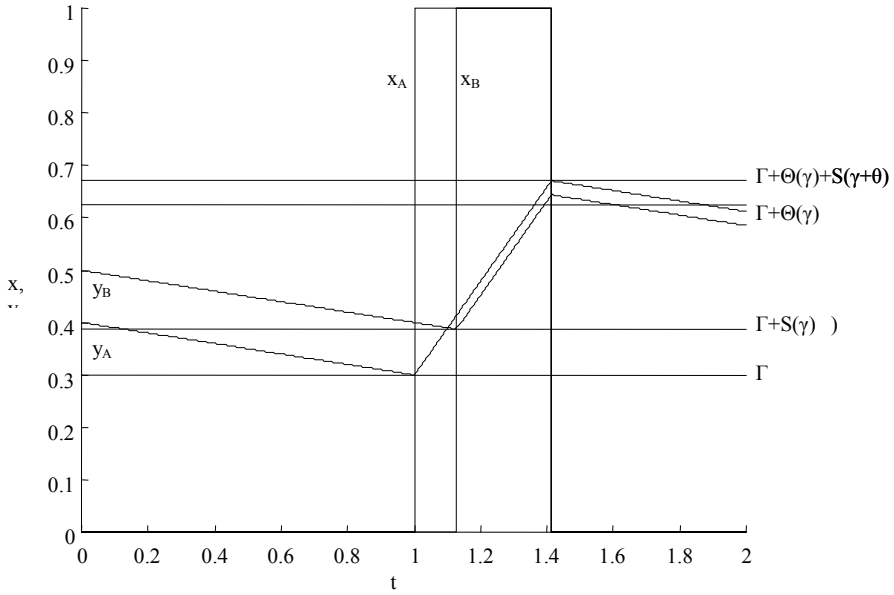

Figure II.8: Temporal evolution of two oscillators *A* and *B*. Integrator y_B and y_A difference shifts its sign after the first jump to the active state. This difference can be reduced (as depicted) or increased after first jump.

Although it may seem that oscillators are desynchronized under these conditions because $|\Delta y(t_1)| > \Delta y(t_0)$ when:

$$\Delta y(t_0) > \frac{p+q}{p-q} S(\gamma) \qquad \text{Eq. II.12}$$

below (*Case VI*) we demonstrate that it is corrected in the next jump from the active state to the silent state and the overall difference after both shifts is reduced.

Case S4:

However, if initial conditions make oscillator *A* to quit the active state before oscillator *B* reaches $\Gamma+S(\gamma)$ in the silent state, excitation is 'forgotten' and there is no variation of Δy, Figure II.9. This boundary is calculated by: $y_A(t_0)=\Gamma$, $y_B(t_0)=y_{B0}$, $y_A(t_1)=\Gamma+\Theta(\gamma)$, $y_B(t_1)=\Gamma+S(\gamma)$:

$$\Delta y(t_0) = S(\gamma) + \frac{q}{p}\Theta(\gamma) \qquad \text{Eq. II.13}$$

Thus, when initial conditions are beyond that boundary there is no synchronization.

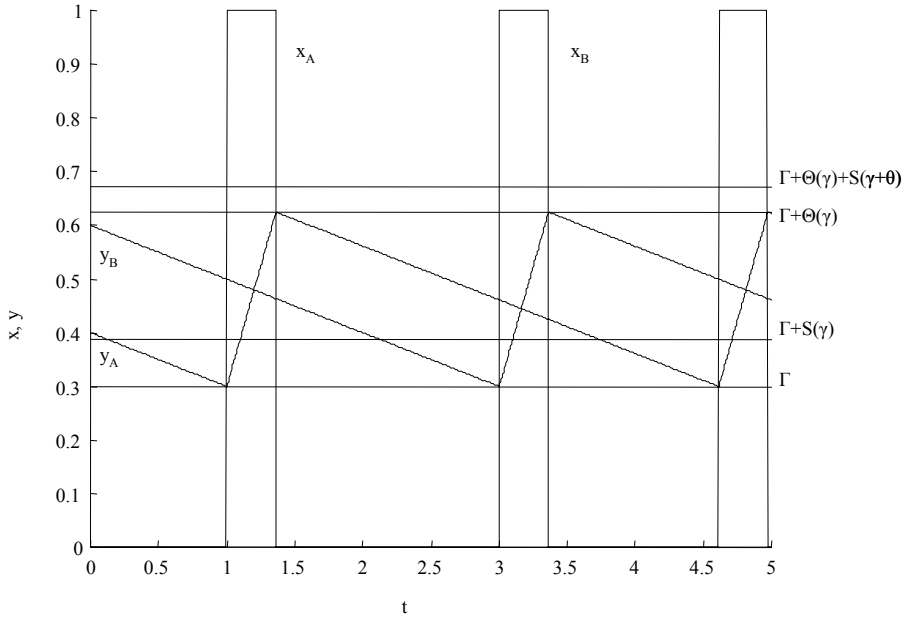

Figure II.9: Temporal evolution of two oscillators *A* and *B*. Integrator state variable difference ($\Delta y(t)$) does not change during the whole cycle.

From active state to silent state:

After the shift from the silent state to the active state studied above, oscillators should come back to the silent state again. Analysis is very similar as the one shown above. We will assume that oscillator *B* precedes oscillator *A* during this period, thus $\Delta y(t)=y_B(t)-y_A(t)$. Let's say that oscillator *B* reaches its high threshold at $t=t_2$ and oscillator *A* reaches its high threshold at $t=t_3$.

Case A1:

If both oscillators are active before y_B reaches $\Gamma+\Theta(\gamma)+S(\gamma+\theta)$ at $t=t_2$, and $y_A(t_2)>\Gamma+\Theta(\gamma)$ (Eq. II.14), then, both oscillators shift to the silent state at the same time, Δy does not vary and they can be considered synchronous. This case is also depicted in Figure II.6.

$$\Delta y(t_2) < S(\gamma+\theta) \qquad \text{Eq. II.14}$$

Case A2:

As seen in case *S2*, if oscillator *B* jumps to the silent state at $t=t_2$ and y_A reaches $\Gamma+\Theta(\gamma)$ later at $t=t_3$, $\Delta y(t)$ will be reduced as:

$$\Delta y(t_3) = y_B(t_3) - y_A(t_3) = \Delta y(t_2) - \left(1+\frac{q}{p}\right)(\Gamma + \Theta(\gamma) - y_{A2}) = \\ = \left(1+\frac{q}{p}\right)S(\gamma+\theta) - \frac{q}{p}\Delta y(t_2) \qquad \text{Eq. II.15}$$

as in Eq. II.9, $\Delta y(t_3)$ is reduced as $\Delta y(t_2)$ increases and there is no sign change until initial conditions force $y_A(t_3)=y_B(t_3)$ (or $\Delta y(t_3)=0$):

$$\Delta y(t_2) = \left(1+\frac{p}{q}\right)S(\gamma+\theta) \qquad \text{Eq. II.16}$$

Case A3:

Eq. II.15 is still valid but the sign of Δy changes from t_2 to t_3 and its absolute value increases as $\Delta y(t_2)$ increases. Note that this case differs from *S3* in that $|\Delta y(t_2)| > |\Delta y(t_3)|$ for any initial conditions because $q<p$:

If $|\Delta y(t_2)| \le |\Delta y(t_3)|$, then:

$$-\Delta y(t_2) \ge \Delta y(t_3) \qquad \text{Eq. II.17}$$

We can substitute $y(t_3)$ by its expression in Eq. II.15:

$$-\Delta y(t_2) \ge \Delta y(t_2) - \left(1+\frac{q}{p}\right)(\Gamma + \Theta(\gamma) - y_{A2}) \Rightarrow \\ \Rightarrow 2\Delta y(t_2) \le \left(1+\frac{q}{p}\right)(\Gamma + \Theta(\gamma) - y_{A2}) \qquad \text{Eq. II.18}$$

As $y_B(t_2)=\Gamma+\Theta(\gamma)+S(\gamma+\theta)$ and $\Delta y(t_2)=y_B(t_2)-y_A(t_2)$:

$$2\Delta y(t_2) \le \left(1+\frac{q}{p}\right)(\Delta y(t_2) - S(\gamma+\theta)) \Rightarrow \\ \Rightarrow \Delta y(t_2) \le \frac{q}{p}\Delta y(t_2) - \left(1+\frac{q}{p}\right)S(\gamma+\theta) < \frac{q}{p}\Delta y(t_2) < \Delta y(t_2) \qquad \text{Eq. II.19}$$

But $q<p$, thus, Eq. II.17, Eq. II.18 and Eq. II.19 are not valid.

Furthermore, next we demonstrate that there is no case *A4* where oscillator *B* reaches its low threshold while oscillator *A* is still active because of the same reason.

Boundary conditions for *case A4* should be:

$$y_B(t_2) = \Gamma + \Theta(\gamma) + S(\gamma+\theta);\ y_B(t_3) = \Gamma + S(\gamma); y_A(t_2) > \Gamma; y_A(t_3) < \Gamma + \Theta(\gamma) \qquad \text{Eq. II.20}$$

Thus, we calculate the time oscillator *B* should take to go from one threshold to the other:

$$\left.\begin{aligned} y_B(t_3) &= y_B(t_2) - q(t_3 - t_2) = \Gamma + \Theta(\gamma) + S(\gamma+\theta) - q(t_3 - t_2) \\ y_B(t_3) &= \Gamma + S(\gamma) \end{aligned}\right\} \Rightarrow$$
$$\Rightarrow (t_3 - t_2) = \frac{1}{q}\left(\Theta(\gamma) + S(\gamma+\theta) - S(\gamma)\right) \qquad \text{Eq. II.21}$$

If we substitute this interval in the expression of $y_A(t_3)$:

$$y_A(t_3) = y_A(t_2) + p(t_3 - t_2) = y_A(t_2) + \frac{p}{q}\left(\Theta(\gamma) + S(\gamma+\theta) - S(\gamma)\right) \qquad \text{Eq. II.22}$$

Boundary conditions force that $y_A(t_2)>\Gamma$, thus:

$$y_A(t_3) > \Gamma + \frac{p}{q}\left(\Theta(\gamma) + S(\gamma+\theta) - S(\gamma)\right) \qquad \text{Eq. II.23}$$

y-thresholds are increased by excitatory coupling $S(\gamma)$ or $S(\gamma+\theta)$ depending on x state variable. If these increases are defined as a function of z-thresholds (Eq. II.6), we can conclude:

$$S(\gamma) > S(\gamma+\theta) \qquad \text{Eq. II.24}$$

But initial conditions in Eq. II.20 force $y_A(t_3)<\Gamma+\Theta(\gamma)$ and also the system should accomplish $p>q$, thus, we obtain a contradiction that demonstrates that oscillator B cannot reach its low threshold while oscillator A is still active:

$$\begin{cases} y_A(t_3) < \Gamma + \Theta(\gamma) \\ y_A(t_3) > \Gamma + \frac{p}{q}\left(\Theta(\gamma) + S(\gamma+\theta) - S(\gamma)\right) > \Gamma + \Theta(\gamma) + S(\gamma+\theta) - S(\gamma) > \Gamma + \Theta(\gamma) \end{cases} \qquad \text{Eq.II.25}$$

Complete cycle

Now, let's look at the complete cycle after shifting from the silent state to the active state and going back to the silent state again. In Figure II.10 we show a graph (return map) representing the final Δy as a function of the initial Δy after the first cycle of the ideal oscillator. Oscillators parameters are γ=0.3, θ=1, s=0.2, k=3.33. In this example, the number of different zones is seven as depicted in figure.

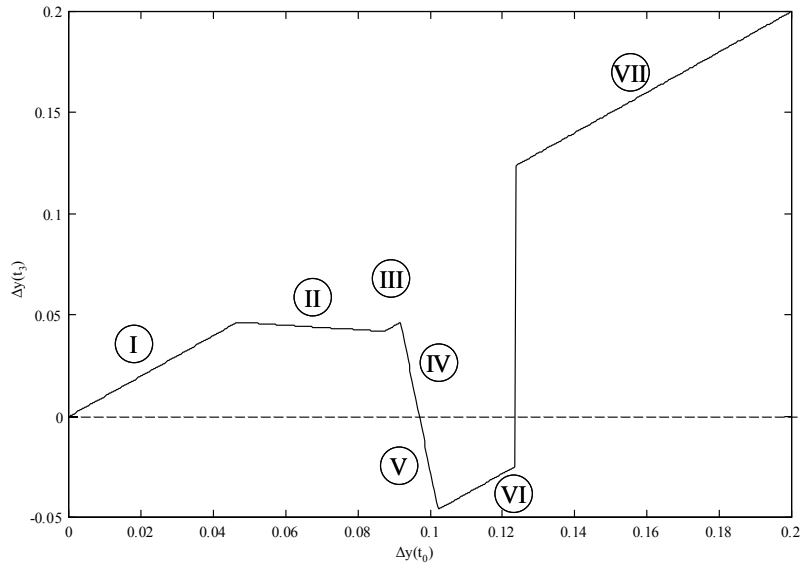

Figure II.10: Return map of two coupled ideal oscillators.

Case I: (cases S1 and A1)

Difference of *y*-variables of oscillators is not reduced, however cells can be considered synchronized because *x*-variables of both oscillators shift simultaneously (Figure II.6). $\Delta y_3=\Delta y_0$.

Case II: (cases S1 and A2 or A3)

There is a difference reduction due to the shift from the active state to the silent state (Figure II.11). However, both oscillators shift from the silent state to the active one simultaneously. $\Delta y(t_3)=f(\Delta y(t_2)=\Delta y(t_0))$ as in Eq. II.15. Note that the combination *S1-A3* is not depicted in the figure because condition for *A3* (Eq. II.16) is not accomplished when case *S1* occurs before and parameters for this example are used –*z*-threshold θ should have been greater.

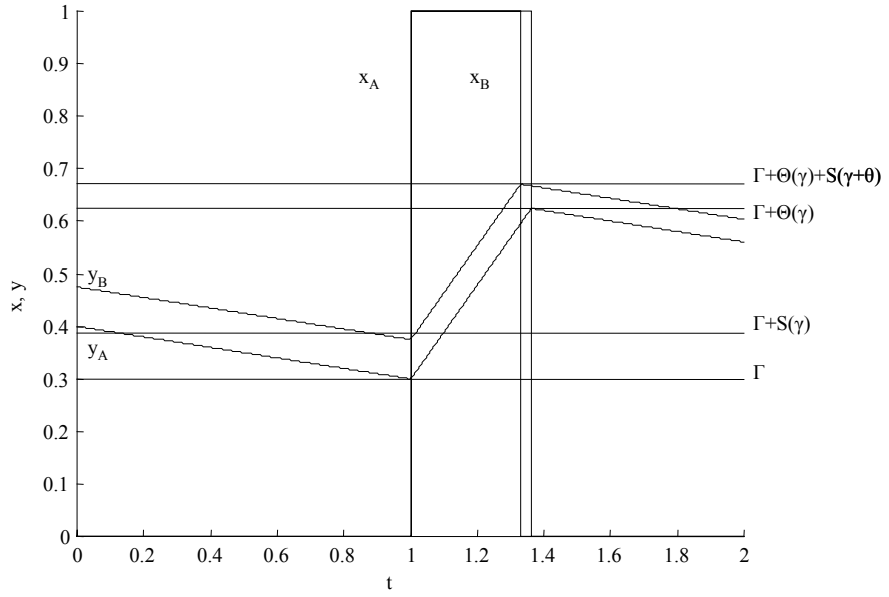

Figure II.11: Temporal evolution of two oscillators *A* and *B*. *Δy(t)* is not reduced after the first shift to the active state but only after the second jump to the silent state.

Case III: (cases S2 and A2)

If there is a reduction of *Δy* in both jumps, $\Delta y(t_3)$ is calculated by Eq. II.10 and Eq. II.15 and assuming that $\Delta y(t_1) = \Delta y(t_2)$:

$$\Delta y(t_3) = \Delta y(t_0) - \left(1 + \frac{q}{p}\right)\left(S(\gamma) - S(\theta + \gamma)\right) \qquad \text{Eq. II.26}$$

Case IV: (S2 and A1)

Δy changes from t_0 to t_1 as in Eq. II.10 and this decrease makes it not to change from t_2 to t_3, thus $\Delta y(t_3)$ is proportional to $-\Delta y(t_0)$ again. The overall effect is that the difference has been reduced (Figure II.7). $\Delta y(t_3)=\Delta y(t_2)= \Delta y(t_1)=f(\Delta y(t_0))$ as in Eq. II.10.

Case V: (S3 and A1)

Threshold that makes $\Delta y(t_1)$ negative (Eq. II.11) has been reached and there is only a diminution of *Δy* in the first jump. Note that $|\Delta y(t_1)| < |\Delta y(t_0)|$ because Eq. II.14 and Eq. II.24 imply that threshold in Eq. II.12 at $t=t_1$ can not be reached.

An example for this case is given in Figure II.8.

Case VI: (S3 and A2)

There is again a reduction in the second jump. It should be stressed that when Eq. II.12 is accomplished, the difference after the first jump is bigger than before it. However, after the second jump, this effect has been corrected. Eq. II.24 and Eq. II.26 demonstrate that $|\Delta y(t_0)| > |\Delta y(t_3)|$, thus oscillators have improved their synchronization as depicted in Figure II.12.

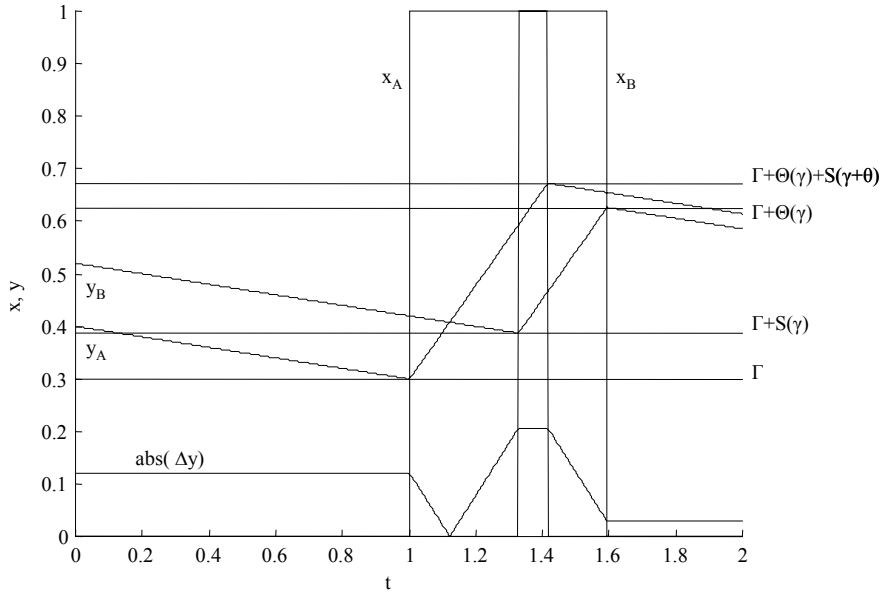

Figure II.12: Temporal evolution of two oscillators *A* and *B*. *Δy(t)* shifts it sign after the first jump to the active state and also increases difference Δy, whose absolute value is also depicted. However, second jump to silent state always reduces this difference, leading to synchrony.

Case VII: (S4)

Δy(t) is too big to synchronize both oscillators. For practical purposes on scene segmentation, this step should be avoided. Thus, we must ensure that the maximum voltage difference in initial conditions is lower than threshold of Eq. II.13.

Values of *Δy* are in the range of [*0,Θ(γ)/2*]. Bigger values can be reduced to this range because *y*-variable of oscillators varies from *Γ* to *Γ+Θ(γ)* when there is no excitation. Thus, this range of possible *Δy* values ($\Delta y(t_0)<\Theta(\gamma)$) and Eq. II.13 implies that *y*-threshold should accomplish to avoid *case VII* for any initial conditions:

$$\Theta(\gamma) < S(\gamma) + \frac{q}{p}\Theta(\gamma) \qquad \text{Eq. II.27}$$

As *y*-threshold is a function of *z*-thresholds as shown in Eq. II.3(c), to avoid *case VII*, exciting synapse value (*s*) must be:

$$s > \left[\left(1-\frac{q}{p}\right)\sqrt{\gamma+\theta}-\sqrt{\gamma}\right]^2 \qquad \text{Eq. II.28}$$

II.2.3 TWO OSCILLATORS PLUS INHIBITOR

We next consider a small network composed of two ideal oscillators without direct coupling and a global cell, which we call inhibitor and have inhibitory connections to both of them.

The inhibitor is a cell that is active when any oscillator or basic cell of the network is in its active state and it is silent when all cells in the network are in their silent state. Connections to the inhibitor to basic cells inhibit oscillations, that is to say, orbits are shifted to lower input z-thresholds by i, thus thresholds become $f^{-1}(\gamma-i)=\Gamma-I(\gamma)$ and $f^{-1}(\gamma+\theta-i)=\Gamma+\Theta(\gamma)-I(\gamma+\theta)$. As excitatory connections do, inhibition also modifies frequency and duty cycle of oscillators.

If we assume that both oscillators are in the silent state, the effect of inhibition is that when one oscillator, let's say A, jumps to the active state, both oscillator thresholds are shifted to lower values. Although it does not affect the oscillator that has already shifted to active, the other one, which we call B and is still silent, will not shift to active until its y_B reaches a lower threshold ($\Gamma-I(\gamma)$) or the other oscillator shifts back to silent. That is to say, low threshold for y_B becomes Γ and y_B is smaller than this.

The overall effect of inhibition is that if oscillators were synchronous, that is to say, their active states have been simultaneous for some time during the period, they become asynchronous. On the other hand, if oscillators were asynchronous, they are kept asynchronous because inhibition is 'forgotten' after the oscillator has come back to the silent state.

If oscillators were directly coupled by excitatory connections and they were stronger than inhibition, the overall result of both effects, which are simultaneous, is that coupling is the difference of excitation and inhibition, i.e. low z-threshold is $\gamma+s-i$ and high z-threshold is $\gamma+\theta+s-i$, leading to a weaker excitation but no inhibition between these cells.

II.2.4 MISMATCH

An important aspect to take into account when designing a physical system is that devices are similar but not identical due to different errors during manufacturing processes. There are different causes that produce this effect known as mismatch and it can be reduced at expense of increasing circuit complexity and size. However, there is always some mismatch that cannot be avoided and algorithms for physical systems must be robust again these little deviations of nominal parameters.

Parameters of the system presented in this chapter that are susceptible of varying between cells are integrator parameters p, q and comparator thresholds γ, θ, s, i. However, these parameters are not appropriate for analysis purposes. These errors will affect basic characteristics of the oscillator as its frequency (f_0), duty cycle (Δ_0) and related characteristics (Eq. II.29) as period (T_0) and the intervals of the period during which the output is active (T_{A0}) and silent (T_{S0}), which are appropriate for the analysis. Thus, we will study the effects of mismatch as a function of variations of these characteristics.

$$\frac{1}{f_0} = T_0 = T_{A0} + T_{S0}$$
$$T_{S0} = \frac{1-\Delta_0}{f_0} \qquad \text{Eq. II.29}$$

In a double oscillator system, mismatches will desynchronize cells because of their different frequency but excitatory coupling can correct these frequency errors provided they are kept small enough.

Above, Eq. II.13 presents a limit for initial conditions to reach synchrony. As in the ideal system, difference of y-variables does not vary between shifts; this condition applies also to the moment just before the first shifts to the active state. Thus, provided initial conditions are synchronous oscillators ($y_A(t_0)=y_B(t_0)$), difference of y-variables due to mismatch before the shift of the first oscillator to the active state ($t=t_0+T_S$) should be smaller than value in Eq. II.13.

Because of mismatch, periods of both oscillators are different (T_{SA}, T_{SB}) and, let's say that oscillator B is slower than A as depicted in Figure II.13. Only temporal evolution during the silent state (case *S4* above) is considered because the equivalent case during the active state (*A4*) cannot exist when $p>q$ as demonstrated in Eq.II.25.

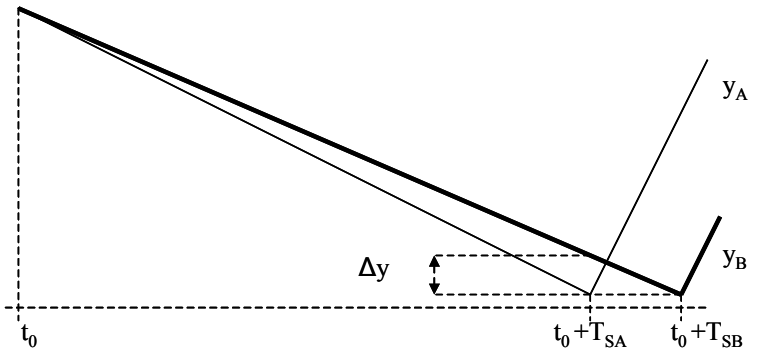

Figure II.13: Evolution of y state variables of two oscillators (osc. *A* thin line, osc. *B* thick line) with mismatch. They are synchronous at the beginning of the silent state and mismatch is responsible of difference y variables at the end of the same state.

Note that for analysis purposes, different y-state variable ranges are equivalent to different slopes with equal y-state variable ranges as we are only interested in the time that an oscillator takes to shift twice. Thus, difference in the slope of y_A and y_B can be the effect of mismatch of q (which affects the slope) but also the effect of mismatch of thresholds Γ, $S(\gamma)$, $\Theta(\gamma)$, $S(\gamma+\theta)$ and $I(\gamma+\theta+s)$ (which affect the y state variable range).

In addition to this, for the network to present computing abilities, various active states should fit in each oscillation period because each different object needs a slot as long as the active cycle of an oscillator to be detected. It implies that oscillator duty cycle should be small ($T_{A0}<<T_{S0}$) , thus, $T_{SB}-T_{SA}=T_B-T_{AB}-(T_A-T_{AA})\cong T_B-T_A=\Delta T$, where the first subscript indicates *A*: active, *S*: silent; and the second subscript, oscillator *A* or *B*.

From Figure II.13, relation between T_{SB} and T_{SA} is:

$$T_{SB} = T_{SA} + \frac{\Delta y}{q} \qquad \text{Eq. II.30}$$

where -q is the slope of the integrator.

As the difference should be smaller than the limit of Eq. II.13, to keep two oscillators synchronous after the first jump, mismatch must be kept below that level where the difference of periods of oscillators A and B (ΔT) is:

$$\Delta T = T_B - T_A \cong T_{SB} - T_{SA} = \frac{\Delta y}{q} < \frac{S(\gamma)}{q} + \frac{\Theta(\gamma)}{p} \qquad \text{Eq. II.31}$$

II.3 OUTPUT DELAY OSCILLATOR

In the previous section, we have analyzed an oscillator whose dynamics are fast enough to assume that its changes are instantaneous. However, when implemented on a physical system, consumption of such an oscillator would be too large due to its fast dynamics. Thus, a more feasible oscillator will have slower comparator dynamics that must be taken into account. In this section we will look at another approximation that considers a comparator output delay, which is a typical secondary effect when cells are implemented with standard CMOS integrated transistors.

First, we will assume that the astable oscillator is modeled as two interconnected integrators with different time constants. A slow one corresponding to the integrator in the ideal oscillator and a faster one that substitutes the hysteresis comparator depicted in Figure II.3.

A block diagram for this oscillator is shown in Figure II.14.

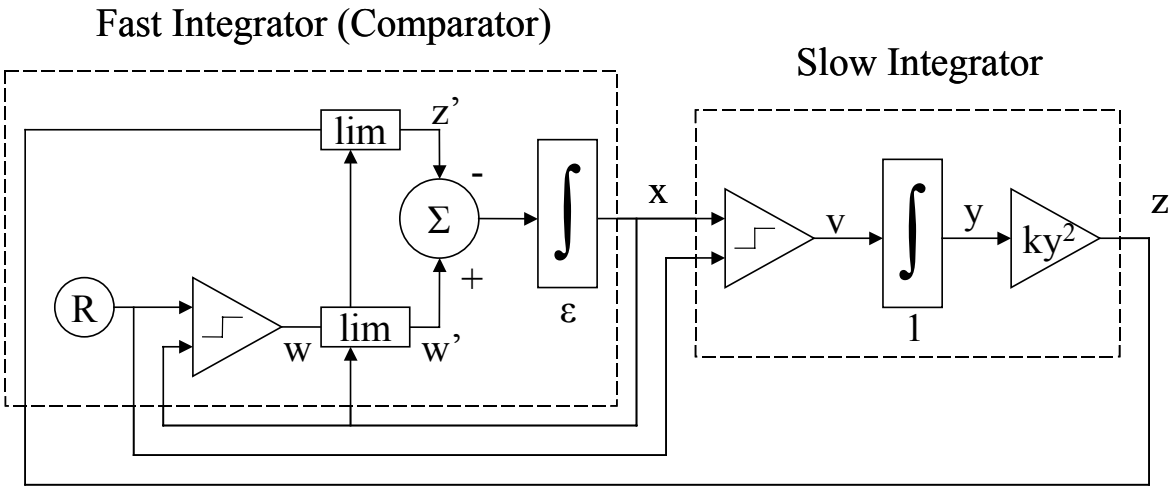

Figure II.14: Hysteresis oscillator with output delay modeled as two integrators with different time constants.

As in the previous model, z and x state variables connect both integrators. z is the same monotonic growing function of y as in the ideal oscillator. Then, this value is subtracted to the output of a comparator (w), which varies with x (Eq. II.34), and the result is integrated by a fast integrator with constant ε (Eq. II.33(a)). In addition to this,

two limiters have been included between variables z and w and the adder. The goal is to limit the fast integrator output, x, from 0 to 1.

This limiters are implemented as shown in Eq. II.32, where variables w' and z' are functions of w, z and x:

$$\begin{cases} w' = w & x < 1 - C \\ w' = w \cdot \dfrac{1-x}{C} & x \geq 1 - C \end{cases} \qquad \begin{cases} z' = z \cdot \dfrac{x}{C} & x < C \\ z' = z & x \geq C \end{cases} \qquad \text{Eq. II.32}$$

where C is a small constant.

Dynamics of both integrator are shown in Eq. II.33:

$$\begin{cases} \dfrac{dx}{dt} = \dfrac{w'(\mathrm{x}) - z'(\mathrm{x},\mathrm{y})}{\varepsilon} & (a) \\ \dfrac{dy}{dt} = v(\mathrm{x}) & (b) \end{cases} \qquad \text{Eq. II.33}$$

Notice that ε<<1 thus, the right-hand side integrator is slower than the left-hand side one if input parameters are on the same order of magnitude.

Although these expressions may seem arbitrary, they are piece-wise linear approximations of the linear and saturation regions of MOS transistors.

To implement a hysteresis cycle and create a positive feedback, w state variable has a small value when output variable, x, is low (that is to say, lower than a reference R) and it is larger when output is high. Difference of both values (w and z) increases integrator output when w>z and decreases this state variable otherwise.

$$w = \begin{cases} \gamma & x \leq R \\ \gamma + \theta & x > R \end{cases} \quad (a) \qquad v = \begin{cases} -q & x \leq R \\ p & x > R \end{cases} \quad (b) \qquad \text{Eq. II.34}$$

When output (x) is lower than reference value R, the slow integrator y state variable decreases at a rate q, though lowering z. This value (z) is subtracted to w, which is smaller than z during this period (w=γ because x is lower than R). When z has decreased enough (z<w=γ), the fast integrator output (x) increases. When it reaches the threshold value, R, the slow integrator state variable increases at a rate p (Eq. II.34b), and z increases. In addition to this, as x>R, w is increased by θ (w=γ+θ), z has decreased below γ during the previous cycle and then increases until it is bigger than w=γ+θ. Then, w becomes bigger that z and x decreases. When the output state variable reaches R, w is decreased to γ, which makes the fast integrator decrease even faster, the slow integrator also decreases at rate q and the cycle starts again.

Evolution of output variables x and y through time for values: p=0.9, q=0.1, w=0.3+1*(x>1); z=3.33*y^2, ε=0.165, is given in Figure II.15 and the orbit in Figure II.16.

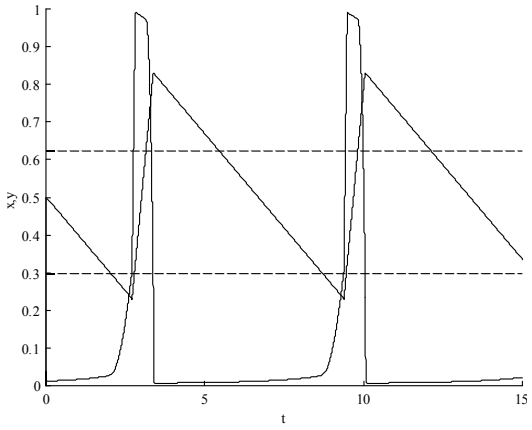

Figure II.15: Evolution through time of x and y of a single oscillator. y-threshold values are Γ=0.3 and $\Gamma+\Theta$=0.62 are also depicted with dashed lines. Note that y range is not limited to thresholds (dashed lines) in this figure neither in Figure II.16 due to output delays.

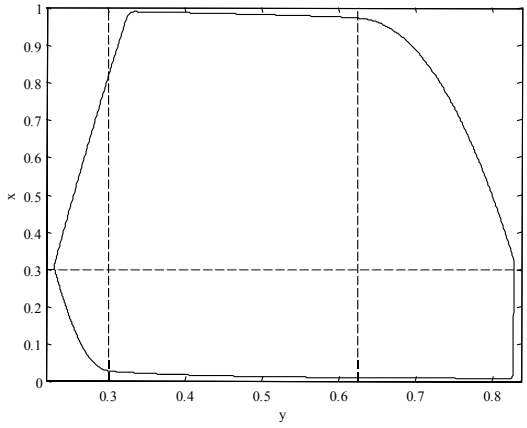

Figure II.16: Orbit of a single oscillator. y-threshold values (Γ=0.3 and $\Gamma+\Theta$=0.62) and reference value (R=0.3) are also depicted with dashed lines.

First, if $x<C$ or $x>1-C$, dynamics mainly depends on the slow integrator because changes in the output variable are slower. Figure II.17 shows limiter curves of the output stage when $z>w$ and Figure II.18 shows the same curves for $w>z$. If dynamics of the output variable can be neglected because shift from the active state to the silent state or vice versa has been done some time before, the final value is the intersection of both curves, where zero input is fed to the integrator.

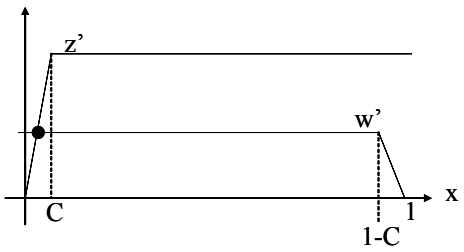

Figure II.17: z' and w' *vs.* x plot when $w<z$

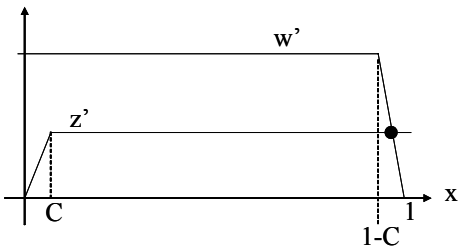

Figure II.18: z' and w' *vs.* x plot when $w>z$

The cross-point in Figure II.17 is the solution of $x=C\,w/z$, shown in Eq. II.35:

$$\begin{cases} y(t) = -qt + y(t_0) \\ x(t) = C\dfrac{w}{z} = \dfrac{C\gamma}{ky^2(t)} \end{cases} \qquad \text{Eq. II.35}$$

However, when the output has to shift from C to $1-C$, difference $w-z$, which is small at the beginning of the shift, must change state variable x. Although dynamics of x is much faster than dynamics of y by a ε factor when inputs of both integrators are on

the same order of magnitude, their dynamics are comparable when *x* has to shift from *C* to *1-C* with a small input to the integrator. Thus, the system should be studied as it were composed by two integrators. Details on oscillator temporal evolution are presented in Appendix A

Nevertheless, as we are mainly interested in some characteristics of the oscillator as frequency, duty cycle and delay when thresholds are reached, there is no need to compute the exact form of the output voltage. Only crossings through *R* are important because they mark the shift from the active state to the silent state. Thus, for analysis purposes, delay oscillator is very similar to the ideal oscillator except some delay to reach thresholds. These thresholds, Γ and $\Gamma+\Theta(\gamma)$, have shifted to Γ_{-D} and $\Gamma+\Theta(\gamma)_{+D}$ respectively (Figure II.19). They can be calculated by equations presented in Appendix A.

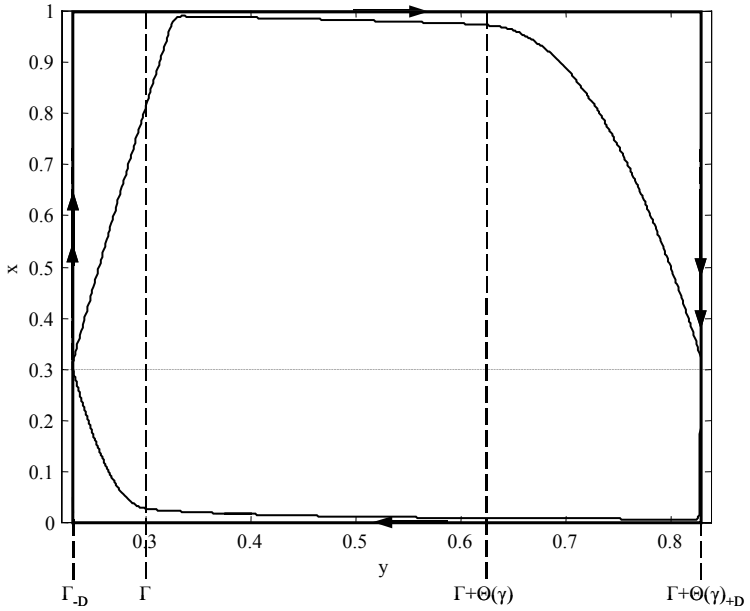

Figure II.19: Orbit of the delay oscillator (thin line) and its simplification for analysis purposes (thick line). Thresholds have changed to Γ_{-D} and $\Gamma+\Theta(\gamma)_{+D}$.

II.3.1 COUPLED OSCILLATORS

Now, we will look at two coupled oscillators and the way they synchronize via excitatory connections. The two-oscillator (*A* and *B*) system we are going to analyze is described by:

$$\begin{cases} \dfrac{dx_A}{dt} = \dfrac{w_A(\mathrm{x_A}) + s_A(x_A, \mathrm{x_B}) - z_A(\mathrm{x_A}, \mathrm{y_A})}{\varepsilon} & (a) \\ \dfrac{dy_A}{dt} = v_A(\mathrm{x_A}) & (b) \\ \dfrac{dx_B}{dt} = \dfrac{w_B(\mathrm{x_B}) + s_B(\mathrm{x_B}, \mathrm{x_A}) - y_B(\mathrm{x_B}, \mathrm{y_B})}{\varepsilon} & (c) \\ \dfrac{dy_B}{dt} = v_B(\mathrm{x_B}) & (d) \end{cases} \qquad \text{Eq. II.36}$$

where parameters are similar as in Eq. II.33 and subscripts *A* and *B* indicate which oscillator we are referring to. The new element added in these equations is the excitatory connection *s*. This element, as in ideal oscillators, is responsible of shifting comparator thresholds to higher values, i.e. moving the orbit of the excited oscillator to the right, when the exciting one is in its active state. It should be noted that these excitatory connections modify the hysteresis cycle of the oscillator, thus varying the orbit, the range of *y* and the oscillatory frequency but not the range of *x*, which is still limited by the non-linear limiters.

Let's now examine the behavior of these two oscillators.

If both oscillators are synchronized, they will remain synchronized as $x_A=x_B$ and *y*-thresholds will shift from $\gamma+\theta+s$ to γ and vice versa simultaneously for both oscillators. Thus, behavior will not change from that of a simple oscillator with $\theta'=\theta+s$, where θ' is the new hysteresis width.

On the other hand, if oscillators are desynchronized, they should synchronize in some oscillations if their initial difference is smaller than a certain threshold.

In Appendix A, we demonstrate that a delay oscillator with no excitation is equivalent to an ideal oscillator with different thresholds for *y*-variable. When an excitation is added, however, the comparison is not so easy because, although equations presented in appendix A are still valid, initial conditions for each zone differ. The trailing oscillator can change from one zone to the next one when it reaches thresholds or when excitation changes these thresholds. It affects equivalent thresholds, reducing the range of *y* due to its quadratic relation with *z* ($\sqrt{a}-\sqrt{b} > \sqrt{a+c}-\sqrt{b+c}$).

However, this effect improves synchronization because the reduction of the range of *y* speeds up the trailing oscillator, thus the difference of both oscillators is also reduced. This property is shown in the return map of two coupled oscillators (Figure II.20) Parameters are the same as in Figure II.15 and s=0.2. Also, a comparison to an ideal oscillator with $\gamma_{(\mathrm{ideal})}=\gamma_{-D(\mathrm{delay})}$ and $\gamma+\theta_{(\mathrm{ideal})}=\gamma+\theta_{+D(\mathrm{delay})}$ is presented in the same plot.

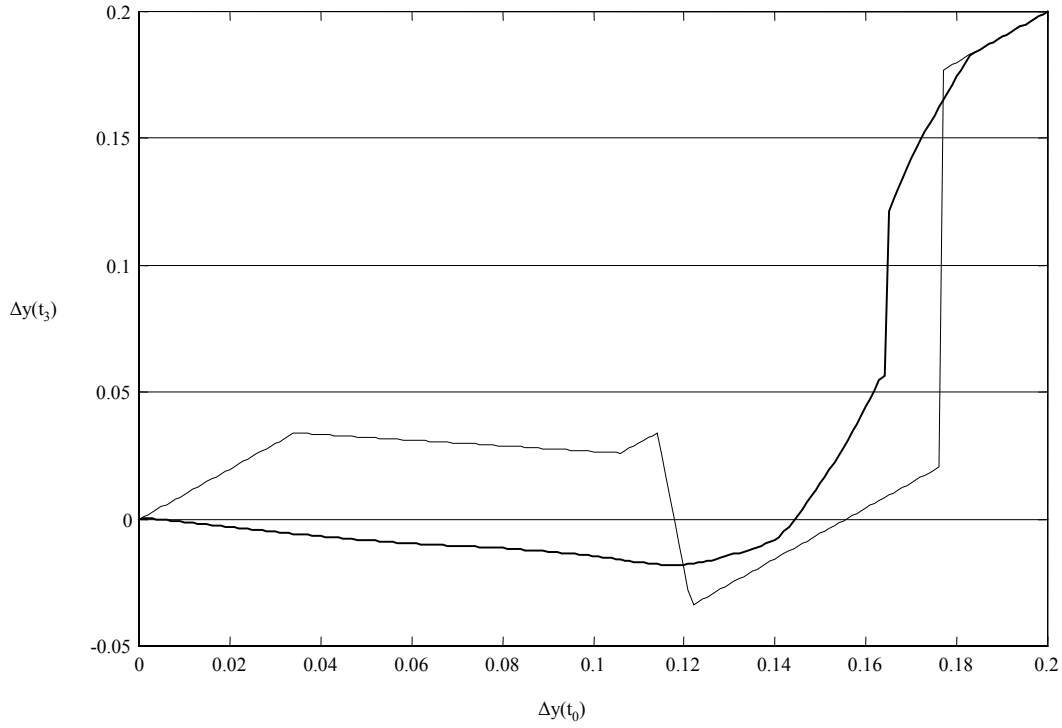

Figure II.20: Simulated **r**eturn map of two coupled delay oscillators (thick line) and two coupled ideal oscillators (thin line). Synchronization occurs below an initial *y*-difference of 0.18 approximately for both of them.

However, Figure II.20 shows that both oscillator schemes, in spite of being very similar and synchronizing when initial conditions are confined to similar ranges, output delay oscillator scheme synchronizes faster than ideal oscillator model. Fast integrator dynamics explains this behavior. When the leading oscillator of two coupled output delay oscillators shifts to active, its fast integrator output increases very slowly because difference of w and z is small after z has reached low threshold. This difference remains small until output state variable x equals reference R, then, thresholds change, w increases from γ to $\gamma+s(\gamma)$ and difference of w and z suddenly increases the same amount $s(\gamma)$. In addition, the slow integrator stops discharging at rate q and starts charging at rate p. Also, when state variable x of the leading oscillator reaches reference R, its excitatory coupling to the other cell makes z-threshold of the trailing oscillator sharply change from γ to $\gamma+s(\gamma)$, which makes its output state variable increase faster and reach reference R faster than the leading oscillator did. Then, the slow integrator changes its slope from $-q$ to p and difference of y state variables of both oscillators is reduced.

We conclude that delay produced in the fast integrator (comparator) improves the capability of synchronization of coupled oscillators.

II.3.2 MISMATCH

Above, we have stated that mismatch is unavoidable in real systems. Hence, any oscillatory network model focused to a physical implementation as ours must consider this. Also, we have stated that errors in different parameters can change some basic characteristics as frequency and duty cycle and it is not important which exact parameter changes but its effects on these two basic properties. For this reason in this section, we are only considering mismatch in one characteristic and not in each parameter. In our experiments, we changed frequency by changing the discharge slope of the slow integrator (q) of one oscillator to study its effects on synchronization.

Oscillators started in a state of synchrony and frequency mismatch was the only responsible for desynchronization after some cycles in the steady state (we took 9 cycles in our experiments). Oscillator parameters are the same as used in examples above except discharge slope of the slow integrator for one oscillator that has been changed from 0.078 to 0.099, which corresponds to a period mismatch from 1% to 28% (Eq. II.37). Mismatch above these values have not been used because they led to asynchronous solutions.

Results are presented in Figure II.21 and Figure II.22. They show the difference of integrator voltages ($\Delta y = y_A - y_B$) after some cycles in the first plot and, in the second one, the lag between rising edges of output state variables (x); both of them as a function of period mismatch. This mismatch is defined as:

$$\frac{\Delta T}{T} = \frac{T_V - T_C}{T_C} \qquad \text{Eq. II.37}$$

where T_V is the period of the oscillator whose q parameter varies from 0.078 to 0.099 and T_C the period of the other oscillator whose q parameter does not vary. Note that actual periods are equal as oscillators are synchronous, thus value T_V is referred to the period that would be as if there were no coupling.

Obviously, for large mismatch, synchrony is not possible for any combination of parameters and results are not presented. However, this mismatch limit is quite large and even big variations of periods (28% in out experiments) may lead to synchrony. The main problem for synchronization purposes is the lag between rising edges of oscillators. Simulations (Figure II.22) show that this delay can reach a value around 50% of the active cycle (0.4 delay for a 0.7 active cycle). This delay may cause some problems when oscillators are implemented in a segmentation system and should be minimized. Thus, even oscillators synchronize for big mismatches and low exciting currents; errors must be kept small enough for a successful segmentation result.

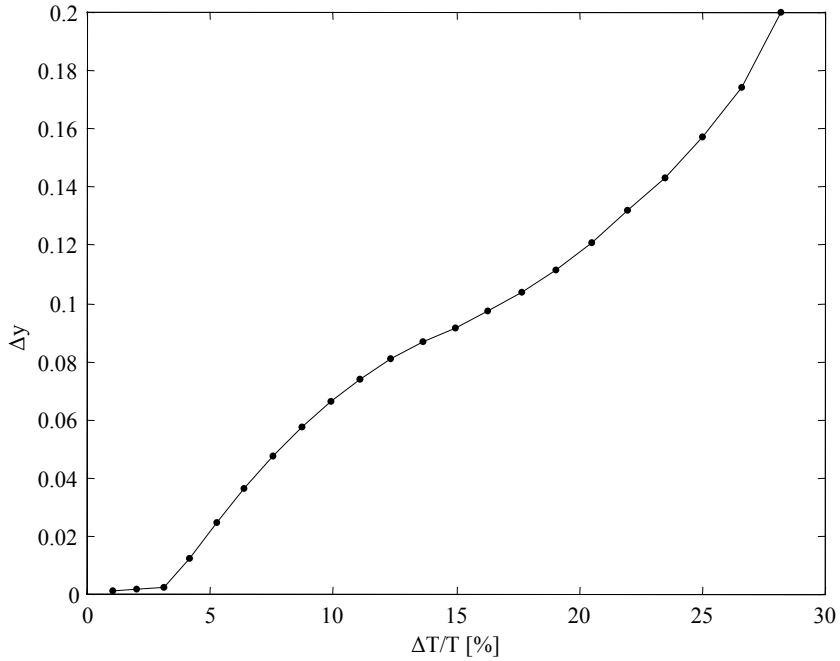

Figure II.21: Variation of differences of y ($\Delta y=y_A-y_B$) for two coupled oscillators as a function of period mismatch (ΔT/T). Oscillators have been considered synchronous at the beginning and mismatch is the only responsible of producing this difference at the steady state.

An important result arises at this point. Delays between oscillators are due to their output delay an also their mismatches. Two coupled delay oscillators with exactly the same parameters, as proven above in the return map of Figure II.20, reach a nearly perfect synchrony in spite of their output delay. However, when the effect of mismatch is considered in such a system, delay between oscillators can be important depending on mismatch value. In addition, this is important when oscillators are part of oscillatory scheme such as the one presented in section II.1.

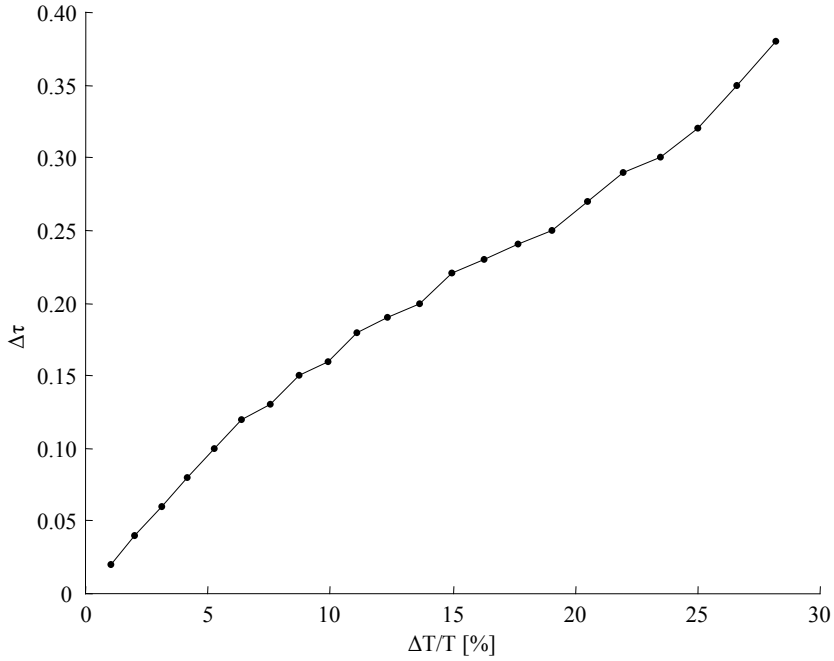

Figure II.22: Lag between rising edges of two coupled oscillators in function of mismatch of periods. As in Figure II.21, oscillators start synchronous and mismatch is the only responsible for the lag. As the active pulse width is 0.7s, both pulses are simultaneously active at least the 50% of this period for a 28% period mismatch.

II.3.3 INHIBITOR

As excitatory coupling, inhibitory coupling or inhibition in the delay oscillator, is performed by subtracting an inhibition term (i) to Eq. II.33(a), thus lowering thresholds. As in the ideal oscillator, a global cell is responsible of activating that inhibition term for all cells in a network when any cell of the network is active. That is to say, its output state variable is higher than a reference (R_A).

Obviously, as we are interested in this inhibition only to affect cells that are not connected, its value should be smaller than excitation to keep its difference positive and thus preserve synchronization properties.

II.4 NETWORKS OF COUPLED OSCILLATORS

The concept of synchronization of two coupled oscillators can be extended to n-dimensional networks of locally coupled oscillators. Although not being connected each cell to all other cells, synchronization may propagate through the network.

The main difference between two coupled oscillators and a network is that in the latter, each oscillator is connected to one or more oscillators depending on network dimensions and its position in the net. To improve synchronization, synapses are

normalized, thus, the sum of all excitatory values that each oscillator receives is the same when all coupled neighbors are active.

Neighborhood must be also defined in each network; thus, oscillator coupling is spread only to a certain radius. However, in spite of coupling being local, global synchronization is possible because each cell that belongs to the same object is coupled at least to another cell. This coupling synchronize both cells that in turn are synchronous to other cells of the object, spreading synchrony throughout all oscillators in the object.

Finally, a global cell that inhibits oscillators is also defined. This element is connected to each other cell and it is active when any oscillator of the net is active, that is to say, its output state variable is higher than a certain threshold. In addition, it is silent when all cells in the net are silent. Since all oscillators belonging to the same object are directly or indirectly coupled, the global inhibitor only adversely affects synchronization. However, it is interesting to study this cell because of its importance in the segmentation scheme.

Analysis of networks of oscillators quickly becomes impractical due to the large number of possible parameters and initial conditions leading to a significant increase of possible solutions. For this reason, the rest of the thesis is based on numerical simulations.

II.4.1 CHAINS WITH NO INHIBITION

Now, let's examine the behavior of a 1-dimensional network or chain of oscillators that are locally coupled to radius 1. This is to say; each oscillator n is coupled to its neighbor oscillators $n-1$ and $n+1$, Edge oscillators are only coupled to their single neighbors.

Figure II.23 shows the temporal evolution of a 16 locally-coupled oscillator network. Oscillators start with different initial conditions and easily reach perfect synchrony after four cycles. Parameters used in this simulation are: q=0.1, p=0.9, θ=1, γ=0.3, s=0.5, ε=0.165, k=3.33.

However, synchronization may not be achieved depending on initial conditions and oscillator parameters, especially excitatory currents, as shown in Figure II.24. where parameters are the same but initial conditions are more spread

.

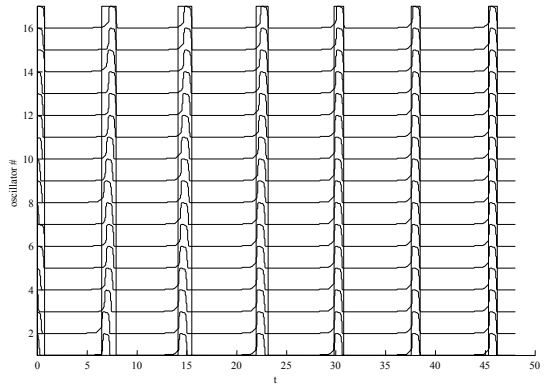

Figure II.23: Temporal behavior of a 16–oscillator one–dimensional network. Thin lines mark periods when any oscillator is active. All oscillators are equal but start with different initial conditions. Note that perfect synchrony is easily achieved after few cycles.

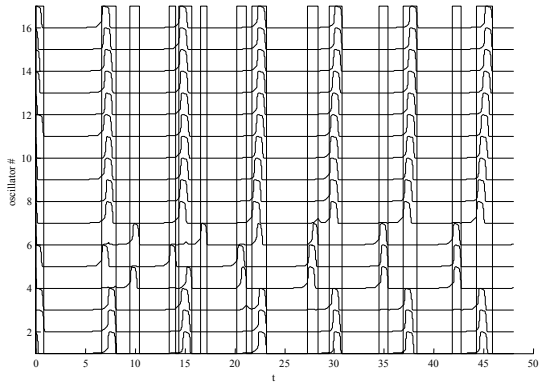

Figure II.24: Temporal behavior of the same network with different initial conditions that prevent the network from synchronizing.

On the other hand, if there is some mismatch in oscillators, perfect synchronization cannot be achieved as in the two-coupled identical oscillator system.

As a global inhibitor cannot be defined in this section, to quantify this synchronization delay concept, let's name as the *network activity state* the time that any oscillator in the network is active. Now, we can define the ratio between the single oscillator active phase to the activity state as:

$$\eta = \frac{T_{Active\ Single\ Oscillator}}{T_{Network\ Activity\ State}} \qquad \text{Eq. II.38}$$

Delays between oscillators and, thus, the network activity state, depend on mismatch. It makes the network activity state be longer than the active phase of a single oscillator. Their ratio (η) can be considered a good quantitative estimation of network synchronization, reaching perfect synchrony when it equals to 1 and worsening as it decreases.

Figure II.25 and Figure II.26 show the effect of mismatch on network synchronization during the transient response and first cycles of the steady state. Parameters are the same as in Figure II.24, but initial conditions are equal for all oscillators and mismatch is considered. Note that indirectly coupled oscillators must not be necessarily active simultaneously as oscillators 1 and 16 in the last period of Figure II.26.

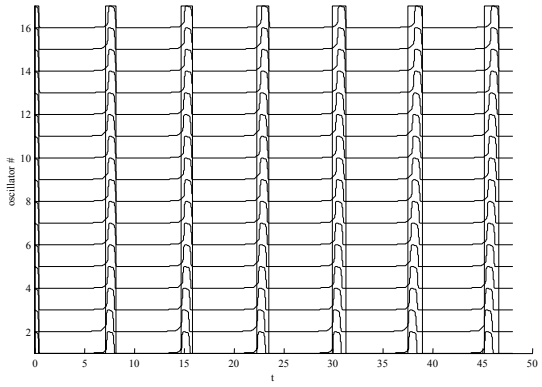

Figure II.25: Temporal behavior of a chain of oscillators with 5% mismatch in the period.

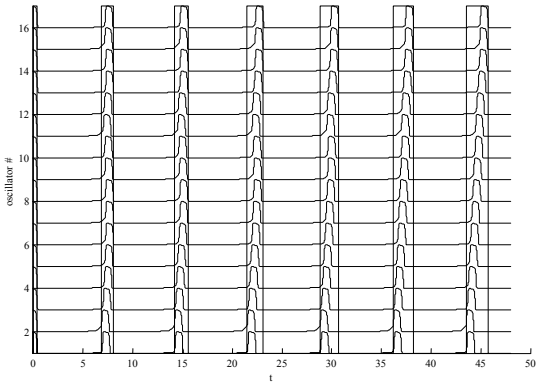

Figure II.26: Temporal behavior of a chain of oscillators with 10% mismatch in the period.

In addition, synchrony depends on oscillator parameters as speed of the hysteresis comparator (ε) and excitation coupling parameter (s). Figure II.27 and Figure II.28 show the effect of these parameters.

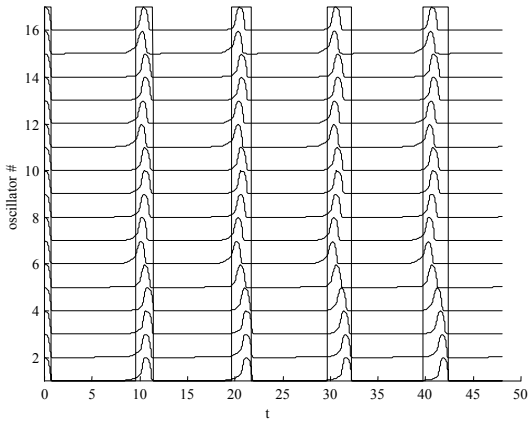

Figure II.27: Temporal behavior of a chain of oscillators with a slow hysteresis comparator (ε=0.66)

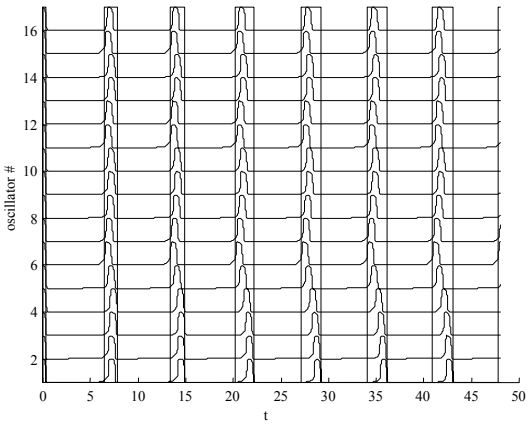

Figure II.28: Temporal behavior of a chain of oscillators with a low exciting parameter (s=0.25)

Both effects presented above (mismatch and different initial conditions), make synchrony more difficult. However, an interesting effect appears when combined, they can improve it; in particular when excitation synapses are strong enough to compensate mismatch, but not so much as to compensate different initial conditions, mismatch compensates the difference in initial conditions. When any oscillator or group of oscillators is no synchronous with other ones, its frequency is slightly different due to mismatch. After some oscillations, their active phases coincide and all oscillators are 'caught' at the same frequency as shown in Figure II.29.

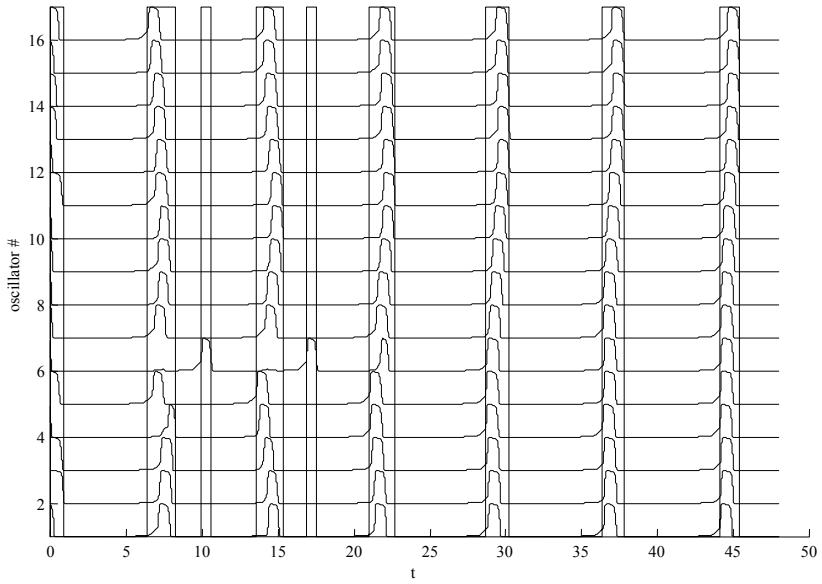

Figure II.29: Combined effect of mismatch and different initial conditions. Parameters are the same as in Figure II.24 and Figure II.25 but the combined effect leads to synchrony.

II.4.2 CHAINS WITH INHIBITION

When the inhibitor is added to the system, only the fastest oscillator and then excited oscillators can shift to the active state because the inhibitor delays non-excited oscillators to shift to the active state by lowering their thresholds. Ultimately no oscillator will shift simultaneously to another one that is not coupled to. The first oscillator to shift will excite its neighbors (one or two, depending whether the oscillator is at the edge of the chain or not). Then after some delay, excited oscillators will also shift to active and afterwards excite their neighbors and so on. Thus, temporal evolution of oscillators will be as depicted in Figure II.30. Note that the fastest oscillator (oscillator 2 in Figure II.30), is the first to shift. Then, it excites oscillators 1 and 3 and so on until oscillator number 16. When oscillator 2 is active, the inhibitor is also active and inhibits all other oscillators.

This figure can be compared to Figure II.26, which uses the same parameters but no inhibition. In addition, global inhibitor activity plays the role of the network activity parameter defined in the previous section. Pulses in the last figure are wider because the overall effect of excitation and inhibition is weaker than the effect of excitation only. In addition to this, synchrony is looser in the first oscillation cycles because mismatch has not spread enough oscillators in Figure II.26 but the inhibitor did in Figure II.30.

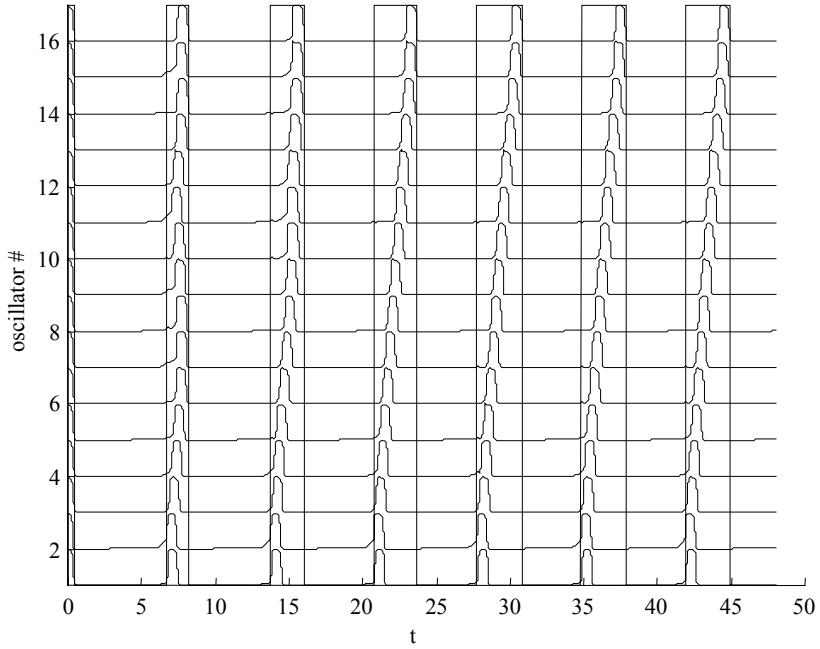

Figure II.30: Temporal evolution of a chain of oscillators with 10% mismatch and an inhibitor with strength *i*=0.1.

II.4.3 2D-BLOCKS OF COUPLED OSCILLATORS

A 2-dimensional block of 4x4 locally coupled oscillators plus an inhibitor has been simulated and results are shown in Figure II.31. Radius of excitatory coupling neighborhood is 1 as in the 1-dimensional block, thus, each oscillator of row *m* and column *n,* (*m,n*), is coupled to its nearest neighbor oscillators (*m-1,n*), (*m+1,n*), (*m,n-1*) and (*m,n+1*). Parameters are the same as used in previous figures but excitation is weaker (*s*=0.25) to slow down synchronization and show it in more detail. Although the number of oscillators is the same as in the 1-dimensional block shown above, the 2-dimensional geometry of this net has more connections than the chain and mean distances between oscillators are shorter for the same number of cells. This property has lead to a stronger synchrony in spite of the weaker excitation. From all of this, it follows that chains are more difficult to synchronize than two-dimensional blocks of the same number of oscillators.

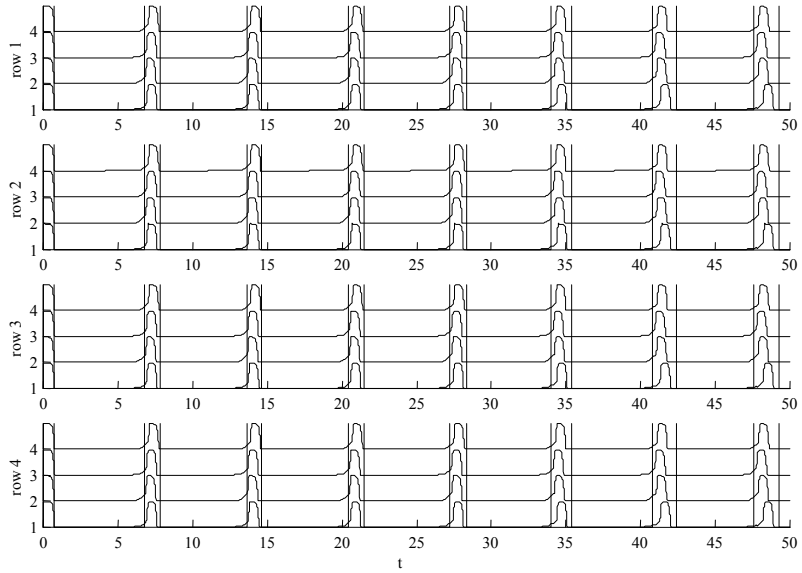

Figure II.31: Temporal evolution of oscillators of a 4x4 network. s=0.25, i=0.1, 10% mismatch

II.5 SEGMENTATION

II.5.1 SEGMENTATION EXAMPLES

We now show some simulations of a 4x4 locally coupled network plus a globally coupled inhibitor. It has been demonstrated that this kind of network can successfully segment images [Wang and Terman'95] [Wang and Terman'97] when they are built of some specific basic oscillators (Eq. II.1).

First, each oscillator is mapped to a pixel of a black and white image. Coupling between oscillators is established depending on their position and pixels property (black or white). Each oscillator of row m and column n (m,n) is coupled to its nearest neighbor oscillators (m-1,n), (m+1,n), (m,n-1) and (m,n+1) provided their pixels share the same property (i.e. both are black or both are white). If they are not mapped to pixels with the same property, neighbor oscillators remain uncoupled. Moreover, coupling is normalized to preserve the same total excitation to all oscillators independently on the number of active couplings. Thus, each individual coupling is obtained by the aggregated coupling for each oscillator divided by the number of coupled oscillators.

Parameters used in these examples are the same as used in Figure II.30. The first example (Figure II.32) is an image of two vertical bars, which are segmented in four cycles. We show the temporal evolution of each oscillator, in the plot. Oscillators that are mapped to pixels that belong to the white bar are depicted at the top, and oscillators that are mapped to pixels that belong to the black bar are depicted at the bottom. Global inhibitor activity is also shown as high pulses that envelope oscillator pulses in each plot.

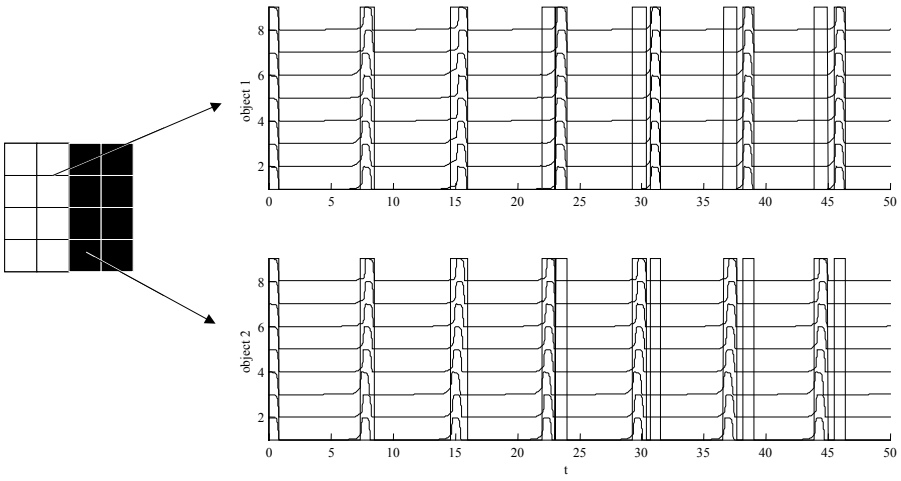

Figure II.32: Temporal evolution of the 4x4 network. The original image to be segmented is shown at the left.

Segmentation results can be easily extracted if oscillator activity of the whole network can be read at a certain time as depicted in Figure II.33. From this figure, it can be seen that active oscillators at t=44.4 belong to an object (black bar) and oscillators that are active at t=46, belong to the other object (white bar).

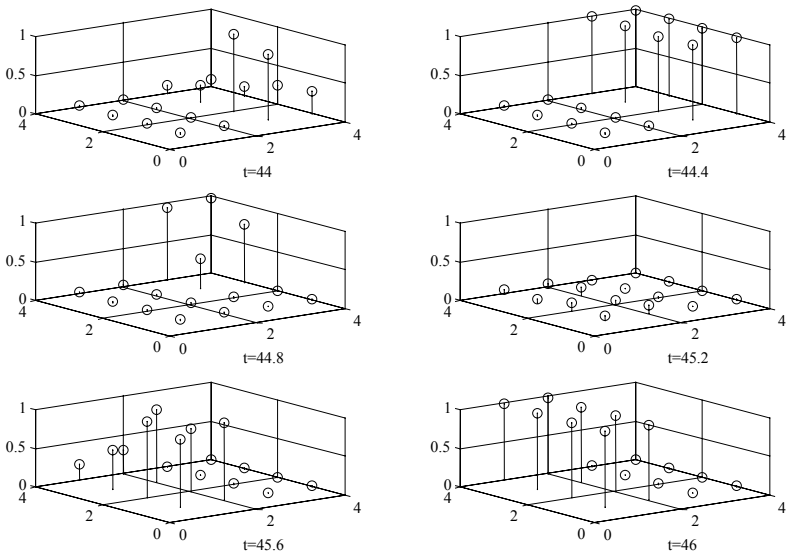

Figure II.33: Network state at different instants. Vertical bars show the output level (from 0 to 1) of each oscillator.

Next example shows the results of segmenting a more complex image built of two black triangles plus the white background. Temporal evolution of all oscillators is depicted in Figure II.34. This simulation shows that objects are also segmented at fourth oscillation.

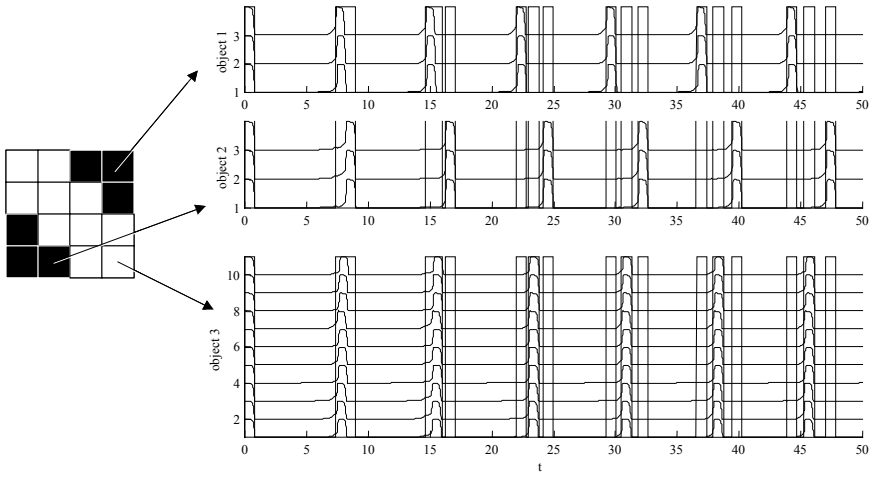

Figure II.34: Temporal evolution of the 4x4 network. The original image to be segmented is shown at the left.

Figure II.35 shows the network state of the whole network at different instants. From this data, pixels that belong to different objects can be easily grouped. Active oscillators at t=44.4 belong to the upper right triangle, active oscillators at t=47.6 to the lower left triangle and active oscillators at t=45.6 are mapped to the background.

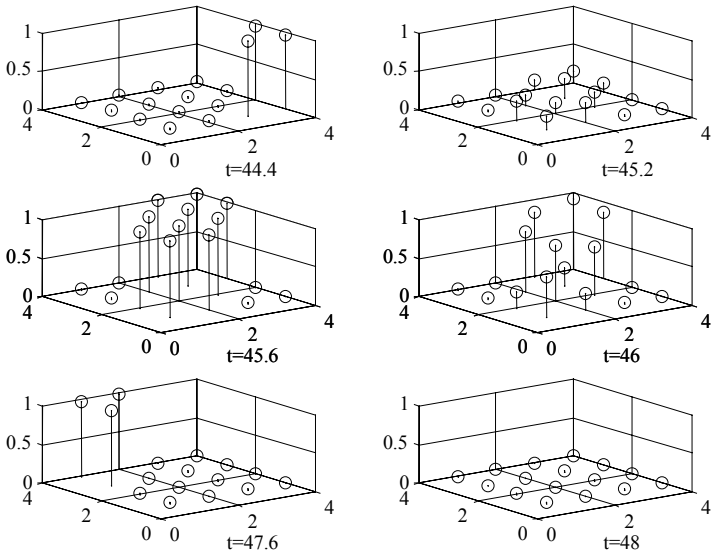

Figure II.35: Network state at different time instants. Vertical bars show the output level (from 0 to 1) of each oscillator.

II.5.2 THE ROLE OF THE INHIBITOR

A key element of the segmentation network is the global inhibitor. Excitatory coupling is responsible of synchronizing oscillators that belong to the same object but it cannot desynchronize them when they belong to different objects. This is the first role

of the global inhibitor. When a group of oscillators that belong to the same object shifts to active, they also activate the global inhibitor, which in turn, inhibits all oscillators of the network. As oscillators of the active group are coupled, excitatory coupling is stronger than inhibitory coupling, thus synchrony in this block is maintained. However, oscillators that belong to different objects and have not yet shifted to active, have no excitatory coupling, therefore, they are only inhibited by the global inhibitor and their oscillation is delayed. This leads to desynchrony between blocks, which is maintained thereafter if frequencies for all groups of oscillators are equal. This is because inhibition only affects oscillators when they are close to thresholds and asynchronous oscillators reach their thresholds at different instants.

Nevertheless, if two blocks of oscillators are active simultaneously, oscillators of both of them receive excitatory and inhibitory coupling simultaneously and are kept synchronous in spite of not being mapped to the same object. Then, this state continues in subsequent cycles and no segmentation is possible. To prevent it, as this is an unstable equilibrium state, some models include some white gaussian noise [Wang and Terman'95] [Wang and Terman'97], especially at the beginning of simulations if initial conditions are the same for all oscillators. On the other hand, other effects than noise can lead to the same result, for instance mismatch or different initial conditions, which are always present in physical designs. For this reason, models based on this kind of implementations are more suited to these effects than to white gaussian noise (even this kind of noise is not the only noise component in microelectronic design, thus other noise models should be added).

The second role of the global inhibitor is to keep the synchrony and desynchrony state reached at the beginning and maintain the same frequency for all oscillators. Thus, other circuits are able to read the network result at any time after the initial transitory stage in spite of their need of more than one oscillation cycle.

An important drawback for this condition is mismatch. It is responsible of changing frequencies of oscillators and it makes blocks of oscillators of networks with no global inhibitor, oscillate with slightly different periods. Therefore, the global inhibitor must correct this negative effect of mismatch by forcing the different groups of oscillators to shift to active following the same order. If oscillation frequencies are not very different, any block cannot surpass another block because they should be active simultaneously and the inhibitor will prevent it.

Other secondary effects have not been taken into account. For instance, the global inhibitor only can desynchronize two blocks instantaneously if it is strong enough to stop oscillations (γ-i<0). If it cannot stop them, oscillations are delayed and more than one cycle is needed to desynchronize blocks at the beginning of the process.

In addition to this, when low inhibition and large mismatch are present, they may lead to random synchronization of blocks of oscillators during one period as depicted in Figure II.36 at time t=70.

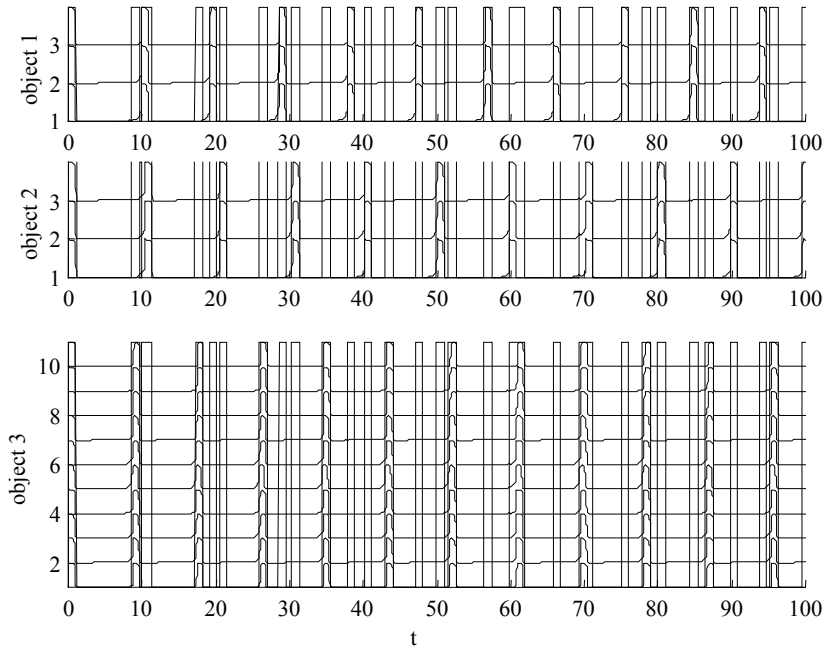

Figure II.36: Temporal evolution of the 4x4 network of Figure II.34 with high mismatch (25%) and stronger excitatory coupling (*s*=1.5). Note that frequency of oscillators mapped to the background (object 3) is higher than other oscillators. This leads to the fact that object 2 and background oscillators are active simultaneously and cannot be distinguished at time t=70.

II.6 DISCUSSION

In this chapter, we have presented a mathematical model for a VLSI oriented non-linear oscillator. We have also shown that a network built of these oscillators is able to segment simple images in few cycles.

First, a preliminary study analyzed dynamics and demonstrated analytically and also using simulations that two ideal and identical astable oscillators synchronize provided initial conditions are close enough. We have also demonstrated that these oscillators synchronize in spite of having some mismatch and we have given a boundary to this mismatch to allow synchrony.

Then, a more accurate model of the electronic oscillator, which we have called output delay oscillator, has also been studied. We have presented in this chapter and in appendix A, a mathematical model for this oscillator, its main characteristics and its temporal evolution. Simulations have shown that two coupled output delay oscillators synchronize under the same conditions than ideal oscillators with equivalent parameters do. Equivalency of parameters of both oscillators is given in Appendix A. Moreover, it has been shown that there is perfect synchrony between two output delay oscillators, in spite of the delay due to the output capacitance. Note that synapse delays have not been considered in this model.

However, when oscillator mismatch is added to the model, some delay between synchronized oscillators appears. If mismatch is too large, it is responsible of desynchronizing coupled oscillators and making their frequencies different. On the other hand, if it is small enough, it prevents the system from reaching perfect synchrony and pulses of the global inhibitor (or network activity) are wider. The main problem of that effect is that not all coupled oscillators are active simultaneously, which may complicate detection of activity by external elements. In addition to this, as delay increases and the activity detection pulse gets wider, the less active cycles can be suited in an oscillation period, the less objects can be segmented. The problem of oscillator delay has been shown in 1-dimensional and 2-dimesional blocks of oscillators. Furthermore, simulations show that delays depend on excitatory synapses strength, oscillator output delay and mismatch.

On the other hand, mismatch effects are not all negative. First, they can help synchrony when initial conditions are not close enough to allow identical oscillators to synchronize. Different frequencies due to mismatch shift oscillator active cycles until they are 'caught' by a block of synchronous oscillators. Then, synchrony is kept provided mismatch is small enough not to desynchronize synchronous oscillators. Secondly, mismatch effects are responsible of desynchronizing blocks of oscillators that are mapped to different objects but randomly synchronous. This is done by white gaussian noise in other models that are not based on electronic implementations.

It has also been shown that inhibition is necessary to desynchronize groups of oscillators that do not belong to the same object but it is also necessary to keep this state until the segmentation result can be read by higher stages. A high boundary for mismatch has been presented.

Finally, a simple 4x4 network of coupled oscillators plus an inhibitor has been used to show segmentation capabilities of the model on simple black and white images.